

Turbine Interaction in Large Offshore Wind Farms

Atmospheric Boundary Layer above a Wind Farm

T. Hegberg
G.P. Corten
P.J. Eecen

ACKNOWLEDGEMENT / PREFACE

This report describes the measurements carried out within the project "Turbine Interaction in large Offshore Wind Farms". This project was supported by the Program Renewable Energy (Programma Duurzame Energie, PDE) in the Netherlands, which is carried out by the Netherlands Agency for Energy and Environment (NOVEM) under the authority of the ministry of economic affairs (Ministerie van Economische Zaken). The contract number is 2020-01-13-10-004 and ECN's project number is 74170. The experimental part of the work is reported in the paper ECN-C-04-048. The measurements were carried out with a model wind farm designed by ECN, in the boundary layer tunnel of TNO, Apeldoorn.

SUMMARY

Background and Aims

Large wind farms are to be expected in the coming decades. We are talking about farms of for example 20 times 20 turbines or larger. Of course it is of utmost importance to be able to predict the production of such farms accurately. However, little is known on cumulative effects of wind turbine wakes. Therefore this project studies the wind turbine interference and especially wake losses for larger offshore farms.

Model

The decrease of the wind speed in the wake of wind turbines can be compared to the frictional drag exerted to the planetary boundary layer by surface roughness. We calculated the effect to the boundary layer when the wind encounters a wind farm. The wind farm was implemented as a sudden change of the surface roughness. Our calculations showed that after an increase of the surface roughness, the wind speed was decreasing up to large distances downstream. Several wind farm models assume that equilibrium is reached after 5 rows of wind turbines, our model showed that it will take at least 10 rows before equilibrium is reached to some extent. This means that our classical models predict a too high power output for really large wind farms.

Experiment

In order to validate the results of the model we set up an experiment in the boundary layer tunnel of TNO, Apeldoorn. We designed and manufactured 30 wind turbines on a scale of 1:400. The turbines are 25 cm diameter and have a hub height of 25 cm. Our design philosophy has delivered rotors which are very similar to full scale rotors regarding the axial force and wake properties, however regarding the efficiency their performance is less. The power coefficient is about 0.30, while it can be between 0.45 and 0.50 for commercial rotors. In the wind tunnel the surface roughness (excluding that due to the wind turbines) was set to sea conditions: after scaling this was approximately 0.2 mm / 400. Sometimes the roughness was adapted to on-shore circumstances as well. We installed several wind farms layouts and measured the wake losses and the effects on the boundary layer.

Results and Discussion

The validation suggests that the wind velocity has not reached its equilibrium value after 5 rows, which indicates that the numerical model can be used for global studies of atmospheric flows above (and behind) large wind farms. The words 'suggests' and 'indicates' were used since the situation in the tunnel was different from the real situation in several aspects. For several reasons the interpretation of the results was difficult. Especially the accurate measurement of the wind speed was a difficulty. A way out for this accuracy problem was the application of differential measurements: we finally set up two farms next to each other in the tunnel.

Conclusion

We can not rely on wind farm models that assume that the wind flow in a farm is stabilized

after five rows of turbines. Many models will over predict production.

Recommendation

We recommend that much attention is to be paid to improvement of the accuracy in the wind tunnel and to the organization of good experiments with actual farms in the field. Both suggestions have been implemented in successive projects, which already have been started.

DISTRIBUTION LIST

Novem	1-4
A.B.M. Hoff	5
C.A.M. van der Klein	6
H.J.M. Beurskens	7
L.G.J. Janssen	8
G.P. Corten	9-10
H.B. Hendriks	11
L.W.M.M. Rademakers	12
P. Schaak	13
T. Hegberg	14-15
P.J. Eecen	16-17
G.J.H. van Nes	18
H. Verkroost	19
Koninklijke Bibliotheek	20
Archive Unit Wind Energy	21-22

EXECUTIVE SUMMARY

Turbine Interaction in Large Offshore Wind Farms

Background and Aims

The worldwide installed wind power increases by about 25% annually. In 2002, this rapid growth has driven the total globally installed wind power to over 31 GW. Much of this power is realized in a few crowded countries such as Germany, the UK or the Netherlands. Since the public acceptance for much more power is becoming a serious drawback, several countries have developed plans for offshore wind energy. For example in the Netherlands the plan is to have 6 GW of wind power installed in the North Sea by the year 2020. Germany, France, Great Britain etc. have similar plans. This means that very large wind farms are to be expected in the coming decades. We are talking about farms of for example 20 times 20 turbines or larger. Of course it is of utmost importance to be able to predict the production of such farms accurately. This means that the wind resource should be known and that we need good models on the interference of the turbines in large farms. Although wind turbine interference can decrease production much, little is known on cumulative effects of wind turbine wakes. One of the largest present offshore farms is Horns Rev, which consists of 10 rows of 8 turbines each. Precise wake farm efficiencies are still confidential for this farm, but numbers in the order of overall efficiencies of about 85% are mentioned. This project studies the wind turbine interference and especially wake losses for larger offshore farms.

Model

The decrease of the wind speed in the wake of wind turbines can be compared to the frictional drag exerted to the planetary boundary layer by surface roughness. The surface roughness is determined normally by an inventory of all obstacles (trees, buildings, etc.) in a certain area and calculating the value for the surface roughness according to certain rules. In this report the surface roughness associated to a wind farm is calculated in a similar way. Subsequently it was calculated what the effect was to the boundary layer when the wind encounters a wind farm. In the models this was implemented as a sudden change of the surface roughness. Our calculations showed that after an increase of the surface roughness, the wind speed was decreasing up to large distances downstream. Several wind farm models assume that equilibrium is reached after 5 rows of wind turbines, our model showed that it will take at least 10 rows before equilibrium is reached to some extent. This means that the classical models predict a too high power output for really large wind farms.

In our model we accounted for thermal effects in a simple manner. Thermal activity in the atmosphere influences the turbulence. A positive temperature gradient in vertical direction (stable atmosphere) decreases turbulence and a strong negative vertical temperature gradient (unstable atmosphere) increases turbulence. This gave us the idea to account for thermal effects by adapting the surface roughness: higher for unstable conditions and lower for stable conditions. Via this trick, our model can estimate the effects of a wind farm for atmospheric conditions including slight departures from neutral atmosphere.

Experiment

In order to validate the results of the model we set up an experiment in the boundary layer tunnel of TNO, Apeldoorn. We designed and manufactured 30 wind turbines on a scale of 1:400. The turbines are 25 cm diameter and have a hub height of 25 cm. The turbine rotors

are two-bladed and look rather different from full scale rotors. The reason is that they are not simple geometric scaled versions of the large rotors of practice. Instead, the rotors are designed in such a way that they have wind turbine wake characteristics, which are similar to those of full scale rotors. When the size of a rotor is reduced from about 100 m to 25 cm, the so-called Reynolds number decreases from about 10 million to just above 25 thousands. In other words, the viscous effects in the flow are much more significant for small rotors. The rotors were designed so that their chord based Reynolds numbers were just above 25.000 since the aerodynamic behavior becomes unpredictable below this value. This was realized by reducing the rotor speed and by increasing the chord. This explains the strange shape of the large chords of the rotor blades. For the airfoils the NACA 0009 was chosen, since this airfoil has a relatively low Reynolds dependency. Despite of those measures to minimize Reynolds effects the airfoils of the models have more frictional drag (loss of energy) and therefore the rotor performance is less than that of much larger rotors.

Our design philosophy has delivered rotors that are very similar to full scale rotors regarding the axial force and wake properties, however regarding the efficiency their performance is less. The power coefficient is about 0.30, while it can be between 0.45 and 0.50 for commercial rotors. The turbines reach an optimum C_p of 0.30 for a pitch angle of $+2.5^\circ$ and a tip speed ratio of 5. This value is very good regarding the small rotor size. From each turbine the rotor speed, the torque, the local wind speed, the power and the axial force could be derived from measured signals combined with calibrations. Six turbines were equipped with strain gauges on the bottom of the tower to measure the axial force. Five different rotors have been manufactured. Those rotors were different regarding the pitch angle, which ranged from -2.5° to $+7.5^\circ$ with step 2.5° . Changing the pitch angle of a wind turbine rotor was carried out by a simple exchange of the rotor. This method yielded accurate and reproducible pitch angle adjustments.

The model results were tested in the boundary layer tunnel wherein the boundary layer was also scaled by a factor 400. The surface roughness (excluding that due to the wind turbines) was set to sea conditions: approximately 0.2 mm / 400. Sometimes the roughness was adapted to onshore circumstances as well. We installed several wind farm layouts and measured the wake losses and the effects on the boundary layer. The latter measurements were collected by a hot wire traverse system that could measure the wind speed at any location with a high sample rate.

Results and Discussion

The validation suggests that the wind velocity has not reached its equilibrium value after 5 rows, which indicates that the numerical model can be used for global studies of atmospheric flows above (and behind) large wind farms. The words 'suggests' and 'indicates' were used since the situation in the tunnel was different from the real situation in several aspects: in the field there is a pressure gradient perpendicular to the wind, while it is parallel to the wind in the tunnel. The expansion of the wake flow is hindered in the tunnel due to the walls and thermal effects could not be investigated in the tunnel. Finally it should be noted that the accuracy of the measurements often was a problem to conclude with definite answers. Especially the accurate measurement of the wind speed was a difficulty. A way out for this accuracy problem was the application of differential measurements: we finally set up two farms next to each other in the tunnel.

Conclusion

We can not rely on wind farm models that assume that the wind flow in a farm is stabilized after five rows of turbines. Many models will over predict production.

Recommendation

Improving the models and experiments regarding the wind farm efficiency of large farms is difficult for several reasons. In the modeling many effects are excluded since they are unknown or very complicated to include. Think of the precise influence of turbulence, thermal instabilities and pressure gradients in the atmospheric boundary layer. Also the effect of turbulence on the power curve of a turbine is not known. Furthermore the effect of the pressure fields and generated turbulence to the boundary layer is not known. Regarding the experiments we also encountered several problems. Very few large wind farms do exist and regarding the few existing ones the data is often confidential or not reliable. The model experiments we have been taken in the tunnel are a way out. However also these experiments have their difficulties: the scaling of the turbines, the blockage of the tunnel and the different thermal effects and different pressure gradients all add uncertainty. It should be noted that the model wind farm we used was built with so much care that it could be used for many different purposes. For example the effects on the power of different types of turbine control or different farm layouts can be tested accurately. Next to this the precise wind speed deficits in the turbine wakes and the generated turbulence can be measured. Such data is valuable input for wind farm design codes and via this way we will come to more reliable codes.

What we finally recommend is that much attention is to be paid to improvement of the accuracy in the wind tunnel and to the organization of good experiments with actual farms in the field. Both suggestions have been implemented in successive projects, which already have been started.

CONTENTS

Notations	9
1 Introduction	11
2 A Wind Farm as Surface Roughness	12
2.1 Problem Formulation	12
2.1.1 Global Force Equilibrium in the Atmospheric Boundary Layer	12
2.1.2 Influence of a Wind Farm on Turbulent Drag Force	14
2.2 Determining the Roughness Length	15
2.2.1 Justification of Roughness Length	15
2.2.2 General Roughness Length Models	16
2.2.3 Roughness Length of Wind Farms: Method of Frandsen	17
2.3 Conclusions	19
3 Effect of Wind Farm Roughness on Planetary Boundary Layers	20
3.1 Derivation of Physical Model and Assumptions	20
3.1.1 Basic Equations	20
3.1.2 Scaling for Relevant Equations	21
3.2 Effects of Temperature and Humidity on Turbulence	23
3.2.1 Physical Considerations	24
3.2.2 Artificial Solution	25
3.3 Physical Model for Numerical Solution	27
3.3.1 Model Equations	27
3.3.2 Initial Values and Boundary Conditions	28
4 Numerical Model	30
4.1 Discretization of the Physical Model	30
4.2 Numerical Stability and Accuracy	34
4.3 Short Model Verification	35
5 Results and Validation	37
5.1 Boundary Layer at Sea	37
5.2 Boundary Layer over Land	39
5.3 Conclusions	41
6 Conclusions and Recommendations	42
6.1 Conclusions	42
6.2 Recommendations	42

References	43
A Initial Paper	44
A.1 Introduction	44
A.2 Roughness Length of a Wind Farm	44
A.3 Surface Parameters Due To a Roughness Change	45
A.4 Estimating the Wind Vector	46
A.5 Results	47
A.6 Conclusions	48
B Computer code	50

NOTATIONS

A	Surface area of wind farm	[m ²]
A^*	Reciprocal of obstacle density	[m ² / turbine]
C_{DN}	Surface drag coefficient for neutral atmosphere	[-]
C_T	Thrust coefficient	[-]
c_{di}	Drag coefficient of local roughness element	[-]
c_t	Generalized thrust coefficient	[-]
D	Rotor diameter	[m]
D_i	Frontal area of wind turbine	[m ²]
F_{CF}	Coriolis force	[N]
F_{PG}	Pressure gradient force	[N]
F_{TD}	Turbulent drag force	[N]
F_{vx}	Viscous force in x direction	[m/s ²]
F_{vy}	Viscous force in y direction	[m/s ²]
F_{vz}	Viscous force in z direction	[m/s ²]
f_0	Coriolis parameter for 45 Northern latitude	[1/s]
g	Gravitational acceleration	[m/s ²]
H	Synoptic scale height	[m]
h^*	Average height of roughness elements	[m]
h_t	Hub height	[m]
I_0	Turbulence intensity	[-]
k	Von Karman constant	[-]
L	Synoptic scale length	[m]
m	mass	[kg]
P_0	Synoptic pressure scale value	[Pa]
p	Pressure	[Pa]
S_L	Total horizontal surface of wind farm	[m ²]
s	non-dimensional turbine distance	[-]
s_s	Frontal cross section of one roughness element	[m ²]
U	Synoptic horizontal velocity scale value	[m/s]
U'	Non-dimensional horizontal velocity	[m/s]
u'	Deviation from horizontal velocity in x direction	[m/s]
u_*	Friction velocity	[m/s]
u_i	Horizontal numerical step value of non-dimensional horizontal velocity	[m/s]
u_j	Vertical numerical step value of non-dimensional horizontal velocity	[m/s]
\mathbf{V}	Velocity vector (u, v, w)	[m/s]
v	Horizontal velocity in y direction	[m/s]
W	Synoptic vertical scale velocity	[m/s]
W'	Non-dimensional vertical velocity	[m/s]
w	Vertical velocity	[m/s]
w'	Deviation from vertical velocity	[m/s]
w_T	Transport velocity of momentum in vertical direction	[m/s]
w_j	Vertical numerical step value of non-dimensional vertical velocity	[m/s]
x	Streamwise coordinate axis	[m]
y	Perpendicular horizontal coordinate axis	[m]
z	Vertical coordinate axis	[m]
z_{farm}	Roughness length of wind farm	[m]
z_0	Roughness before roughness change	[m]
z_{01}	Roughness length after roughness change	[m]

α_c	Constant value in Charnock formula	[-]
Δx	Step size in horizontal direction	[-]
$\Delta \zeta$	Step size in vertical direction	[-]
δP	Synoptic horizontal pressure difference	[Pa]
ζ	Transformed vertical coordinate	[-]
ζ_j	Transformed vertical coordinate at local (vertical) position	[-]
λ_{\max}	Largest eigenvalue of a linear system of differential equations	
μ	Dynamic viscosity coefficient	[kg m ⁻¹ s ⁻¹]
ν	Kinematic viscosity coefficient	[m ² /s]
ρ	Air density	[kg/m ³]
τ	Reynolds stress	[N/m ²]
ϕ	Latitude angle	[°]
Ω	Angular velocity vector	[rad/s]
Ω	Scalar value of Earth angular velocity	[rad/s]

1 INTRODUCTION

This study deals with the influence of large wind farms on the atmospheric boundary layer. Expected is, that such an influence results in a wind direction and wind velocity change above the farm. The present methods taking such effects into account are inaccurate and incomplete. The knowledge resulting from this project will eventually improve the computational methods leading to favourable power production and structural load calculations.

Referring to the project proposition written by Eecen and Hegberg, the atmospheric conditions that hold for wind turbine wakes in wind farms are highly different from freestream conditions. Consequently, power production and structural loads of turbines in wind farms clearly differ from that of stand-alone turbines. A wind turbine extracts energy from the mean flow which causes a velocity deficit around hub height. This results in a decreased energy yield for downstream turbines. In addition, due to the mentioned wake effects the local turbulence intensity increases which results in higher loads on the downstream turbines.

The main goal of this work is finding a computational method that determines a 2-dimensional velocity field above a large wind farm. To achieve this specific goal, several issues should be considered. First of all, the wind farm should be able to interact with the atmospheric boundary layer, which is explained in chapter 2. Secondly, a physical model has to be constructed that determines the development of the velocity field due to the wind farm, as introduced in chapter 3. Chapter 4 considers the numerical solution of the physical model, which is followed by chapter 5 that compares the computational results with the wind tunnel measurements. Finally, chapter 6 draws some conclusions and gives some significant recommendations for improvement of the model.

2 A WIND FARM AS SURFACE ROUGHNESS

2.1 Problem Formulation

This section shows the influence of a changing turbulent friction force on the force equilibrium system in the atmospheric boundary layer. It is assumed that the wind velocity and the wind direction above a wind farm change due to increased surface roughness. This may also have consequences for the wind farm itself. The basic theory, which is mostly based on [7], will be introduced in this section. More detailed explanations of the general theory can also be found in [4].

2.1.1 Global Force Equilibrium in the Atmospheric Boundary Layer

In this paragraph we follow the text of Stull [7]. For this basic consideration only horizontal motion is considered: gravity and hydrostatic pressure gradient cancel each other and therefore can be omitted. The x -axis is aligned with the flow according to a cartesian, right-handed coordinate system where the z -axis points upwards. Further, we assume that the flow has no vertical velocity component. From Newton's second law (the rate of change of momentum, i.e. acceleration, of a particle equals the sum of all forces acting) it follows that steady flow in the atmospheric boundary layer is caused if pressure gradient, Coriolis effects and the turbulent friction are in equilibrium. The forces will be quantified separately.

Pressure gradient

The pressure gradient force per unit of mass, F_{PG}/m , can be determined as follows:

$$\frac{F_{PG}}{m} = -\frac{1}{\rho} \frac{dp}{dy} \quad (1)$$

where ρ denotes the air density and p is the air pressure.

When an atmospheric flow initiates at a wind velocity zero, the pressure gradient force and the wind velocity have similar directions. Due to the fact that air moves with respect to a rotating earth the Coriolis force affects the velocity field until the forces are equal but oppositely directed. When that equilibrium has been reached the flow has turned 90° , which means that the force directions are perpendicular to the flow, see figure 1. The figure shows that the component F' is constantly in the same direction as the wind velocity and the component F'' is directed perpendicular to the velocity vector. Both components result from the pressure gradient force. It must be noted that F' decreases when the wind velocity increases: the flow reaches its equilibrium velocity.

Coriolis effect

The Coriolis force (F_{CF}) is proportional to the velocity of an air parcel and the angular velocity of the earth. The force per unit of mass is given by the vectorproduct:

$$\frac{\mathbf{F}_{CF}}{m} = 2\boldsymbol{\Omega} \times \mathbf{V} \quad (2)$$

in which $\mathbf{V} = (u, 0, 0)$ is the velocity vector where the components follow the cartesian axis system, $\boldsymbol{\Omega} = (\omega \cos \phi, 0, \Omega \sin \phi)$ is the angular velocity vector of the earth, expressed in a local axis system at latitude angle ϕ . Substituting the vectors and evaluating equation 2 yields:

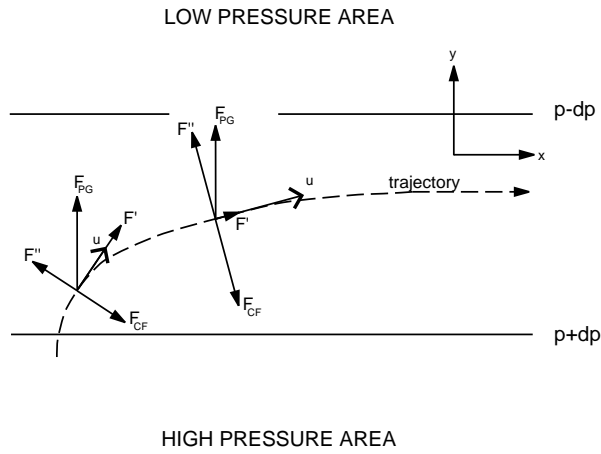


Figure 1: Adjustment to geostrophic balance

$$\frac{F_{CF_y}}{m} = 2\Omega u \sin \phi \quad (3)$$

where, for this case, the latitude angle ϕ can be referred to as the angle between the vectors \mathbf{V} and $\mathbf{\Omega}$. The Coriolis force is perpendicular to the plane that is formed by \mathbf{V} and $\mathbf{\Omega}$.

Turbulent drag

The turbulent drag (TD) force (F_{TD}) can be thought of as a drag force experienced by the air in the boundary layer due to the roughness of the earth's surface, see figure 2.

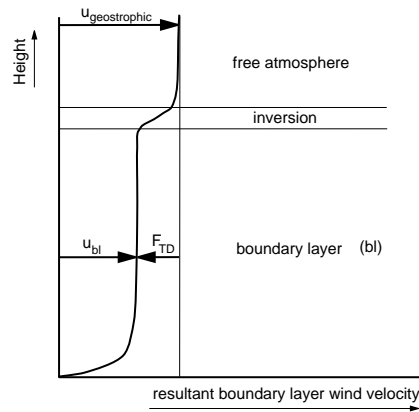


Figure 2: The turbulent drag force in the atmospheric boundary layer, *from: reference [7]*

The drag force per unit of mass is:

$$\frac{F_{TD}}{m} = -w_T \frac{u}{z_i} \quad (4)$$

where w_T is a transport velocity of momentum in vertical direction due to turbulence and z_i is the boundary layer depth. For this moment we only consider a neutrally stable boundary layer, which means that vertical motion due to heating or cooling of the earth's surface is omitted. Finally, neutral conditions indicate that turbulence is primarily generated by wind shear. The vertical transport velocity can be expressed in terms of a drag coefficient:

$$w_T = C_{DN}u \quad (5)$$

where the wind velocity v is positive, and C_{DN} is a drag coefficient that varies from 3×10^{-3} over smooth surfaces to 30×10^{-3} over rough surfaces. The nature of the turbulent drag force is explained more physically in figure 2. From that figure can be concluded that the difference between the resultant boundary layer wind (u_{bl}) and the geostrophic wind ($u_{geostrophic}$) is caused by the turbulent drag force.

Combining pressure gradient, Coriolis and turbulent drag

Geostrophic flows are known to be steady and rectilinear. If the turbulent drag force in figure 3 is neglected, the flow is called geostrophic. When the three forces (including turbulent drag) are in equilibrium, the force system as shown in figure 3 appears. The result of this three-force system is that the wind speed vector crosses the isobars at angle α .

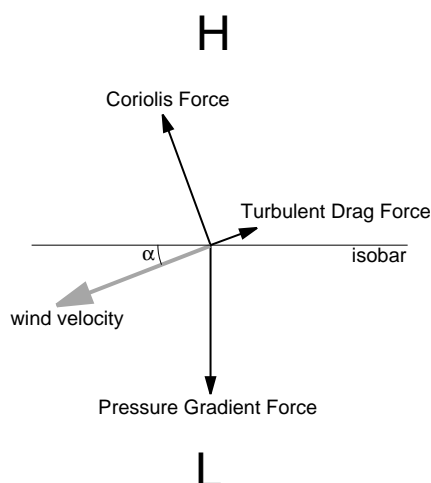


Figure 3: Force equilibrium in the atmospheric boundary layer for rectilinear flow

2.1.2 Influence of a Wind Farm on Turbulent Drag Force

According to [2] atmospheric boundary layer flows experience wind farms as surface roughness. When the roughness changes the turbulent drag force adjusts, which has its effect on the vertical velocity profile. From figure 3 it can be deduced that due to the larger friction force the equilibrium state adapts, affecting the wind speed and angle significantly. Because of turbulent mixing the momentum of larger heights is transported downward.

It is important to have an estimation for the turbulent drag force because it is the main source of momentum input into a large wind farm. One way to estimate that force is to quantify the roughness of the earth's surface. In that case we search for a model that converts a wind farm

into surface roughness and determines the resulting turbulent drag force. In the next section the concept of 'roughness length' will be introduced.

2.2 Determining the Roughness Length

2.2.1 Justification of Roughness Length

Surface roughness causes a turbulent drag force that tends to decelerate the flow. For example, the sea has a smooth surface that generates a force that is less than caused by a land surface. This surface roughness can be expressed in a roughness length, z_0 . The parameter is related to a relative large ground surface: it is an average of roughness element heights and frontal surfaces, with respect to a ground surface. The concept of roughness length appears when the logarithmic wind profile is used. Therefore, the following is assumed:

- The surface layer is approximately 100 m thick (first 10% of the boundary layer),
- The turbulence model assumed is 'mixing length' theory as in reference [6],
- The wind shear is positive (i.e. wind speed increases with increasing height).

In this paragraph, most theory is further based on reference [6]. The turbulent drag force has already been mentioned in the previous section: when the force is translated into a turbulent shear stress at the earth's surface (also referred to as Reynolds stress), the shear stress τ becomes:

$$\tau = \overline{\rho u'w'} = \rho u_*^2 \quad (6)$$

where $\overline{u'w'}$ denotes the vertical turbulent flux and u_*^2 designates the friction velocity. Both quantities are a measure for the Reynolds stress. For neutral atmosphere, $u_* \approx 0.3$, for non-neutral boundary layers the value could be significantly different.

Wind turbines operate most of the time in the surface layer: in that layer the effects of turbulent exchange of momentum are dominant. Only for that particular condition, from mixing length theory and equation 6 the following ordinary differential equation holds:

$$\frac{du}{dz} = \frac{u_*}{kz} \quad (7)$$

The solution is:

$$u(z) = \frac{u_*}{k} \ln \left(\frac{z}{z_0} \right) \quad (8)$$

where z_0 is an integration constant that is frequently referred to as 'aerodynamic roughness length'. It also means, in a more physical way, the height at which the wind velocity has reduced to zero, assuming a logarithmic wind profile.

2.2.2 General Roughness Length Models

In this section some common roughness models for atmospheric sciences will be introduced. The aerodynamic effects of operating wind turbines are still neglected, in this paragraph they behave like normal roughness elements.

Roughness model of Lettau

Lettau [6] describes the roughness length over land as follows:

$$z_0 = 0.5h^* \left(\frac{s_s}{S_L} \right) \quad (9)$$

where S_L designates the total ground surface area, h^* denotes the average height of the elements and s_s is the average frontal cross-sectional surface of one roughness element on the surface S_L multiplied by the number of objects. Physically, this method takes the following into account:

- The height of the obstacle,
- the cross-section of a roughness element as seen by the flow,
- the (reciprocal) 'obstacle density', which is described by the average horizontal area available to each roughness element.

The expression is useful when the roughness elements are evenly spaced, not too close together, (say, 10 times the obstacle height) and similar of shape. It could be used for a roughness calculation of a regular large wind farm if one realizes that the thrust coefficient of a turbine has not been taken into account. One solution could be to include some effects of porosity into the conventional models; porosity indicates that air is able to flow through roughness elements, which affects the behaviour of the flow behind an obstacle. A possible change in flow conditions could be: less turbulence and reduction of the disturbed flow area.

Roughness Model of Charnock

The method described above is only valid for a surface that does not change in time. Since offshore wind energy becomes more important determination of roughness lengths at sea becomes more significant. For sea surfaces a different method is available to calculate the roughness length, which was developed by Charnock [6]. According to his model the roughness depends on the friction velocity u_* :

$$z_0 = \alpha_c \frac{u_*^2}{g} \quad (10)$$

where g and α_c are the gravitational acceleration and an empirical constant ($\alpha_c = 0.00144$) respectively. When the relation of Charnock is combined with the logarithmic wind profile a parabolic relation between the roughness length and the horizontal velocity results, see figure 4. For calculation of the roughness length we need the velocity at hub height (100 m above sea-level), which is also a result of substitution of the logarithmic wind profile (equation 8) into equation 10.

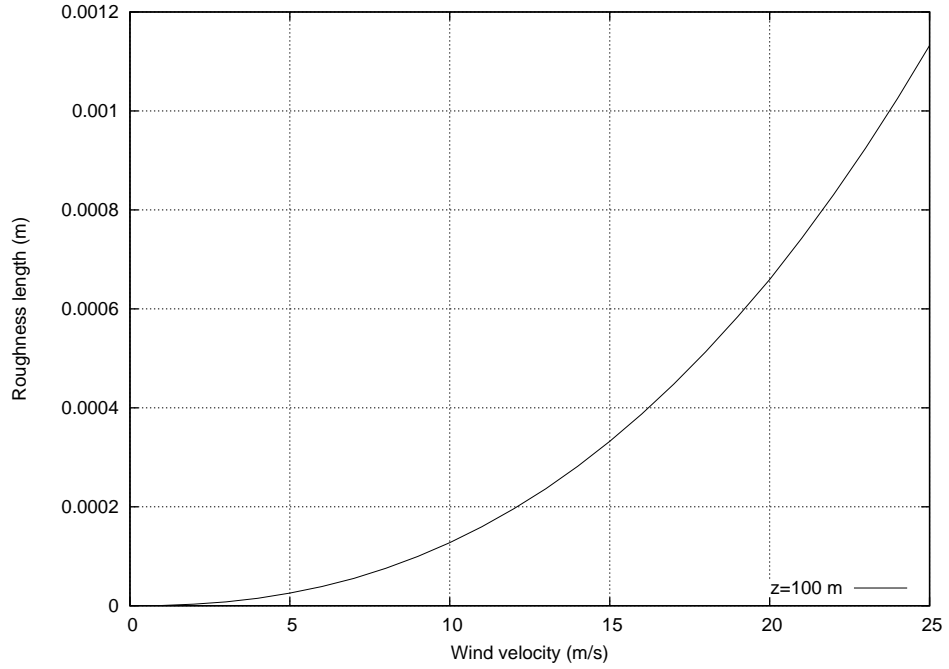


Figure 4: The relation of Charnock, $\alpha_c = 0.0144$

2.2.3 Roughness Length of Wind Farms: Method of Frandsen

Frandsen [3] studied the influence of turbines and took the effect of turbine interaction into account. He included the effect of wind turbine wakes. Using theory and measurements he came to the following formula:

$$z_{0,\text{farm}} = h_t e^{\frac{-k}{\sqrt{c_t + k^2 I_0^2}}} \quad (11)$$

where h_t is the hub height at which the wind speed is measured, c_t is a 'generalised' thrust coefficient which is valid for a group of turbines, I_0 is the turbulence intensity of the undisturbed flow and $k = 0.4$ is the Von Karman constant. The formula may also be used if no wind turbines are present. In that case $c_t = 0$, which gives us the z_0 as would follow from the freestream. When a windfarm is present the c_t obtains a value that depends on the spacing of turbines, type of turbines and the dimensions of the windfarm. The coefficient c_t is constructed as described below. First one considers figure 5 that shows an simplified wind farm.

According to [3] due to the wind farm an additional drag coefficient must be superposed to the surface roughness of the freestream. It is assumed that the wind velocity remains constant within the wind farm, that all turbines are evenly spaced and that all turbines have the same properties. The total wind farm drag coefficient becomes:

$$c_t = \frac{1}{2A} \sum_{i=1}^{N^2} D_i c_{d_i} \quad (12)$$

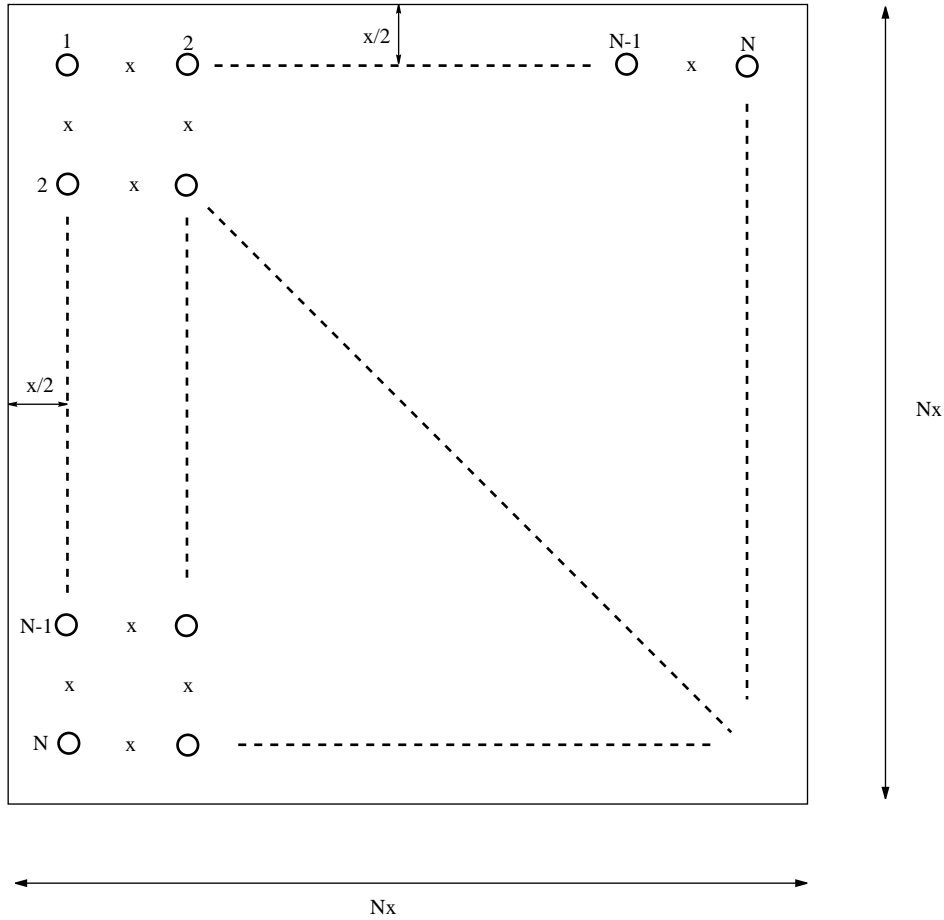


Figure 5: A simplified model of a large wind farm

where A is the total ground area, D_i is the frontal area of a wind turbine (especially the rotor disk surface) seen by the flow and c_{d_i} is the drag coefficient of a single turbine or thrust coefficient. From figure 5 it follows that the distance between the turbines is x , the rotor disk area is $(1/4)\pi D^2$ and the ground area is $N^2 x^2$. This gives:

$$c_t = \frac{1}{8} \frac{\pi C_T}{s^2} \quad (13)$$

where $C_T = 8T / (\rho U^2 \pi D^2)$ denotes the thrust coefficient, where T denotes the drag force caused by the turbine, U is the wind velocity at hub height and ρ is the air density. The symbol s , which may be defined as a non-dimensional turbine distance is written as follows:

$$s = \sqrt{\frac{A^*}{D^2}} \quad (14)$$

in which D is used for the rotor diameter and A^* is written as:

$$A^* = \frac{\text{Total horizontal area of the wind farm}}{\text{Total number of wind turbines}}$$

which is frequently referred to as the average horizontal area available to each roughness element, or (the reciprocal of) the obstacle density.

Since the total drag coefficient of the farm is determined, the relation for the turbulence intensity can be used to find the new roughness length. For a neutral boundary layer over land one uses frequently:

$$C_{DN} = \frac{k^2}{\ln^2\left(\frac{z}{z_0}\right)} \quad (15)$$

If the drag coefficient in equation 15 is replaced by the sum of the farm drag coefficient and that of the freestream, formula 11 appears. Physically, the turbulence intensity is increased by the thrust coefficient, the mutual distance and the number of turbines, which is expressed in a z_0 of the wind farm.

2.3 Conclusions

Not much literature could be found on the modelling of wind farms as surface roughness. The few models were analysed, but it appeared that the effect of wind turbines hardly ever had been taken into account. Still we could approach a wind turbine as a conventional roughness element; the consequences are that roughness lengths appear to be higher because the conventional models all assume that the elements have no porosity. Porosity is a measure that quantifies the ability of a roughness element to allow a fluid or a gas to flow through it. A wind turbine allows air to flow through the rotor, which indicates that such roughness elements have to be treated differently.

Since the common methods of roughness length modelling are not sufficient for using wind turbines as roughness elements, the study made us decide to choose for the method of Frandsen because it takes wind turbine wakes into account. In this model the concept of porosity has not been considered.

3 EFFECT OF WIND FARM ROUGHNESS ON PLANETARY BOUNDARY LAYERS

3.1 Derivation of Physical Model and Assumptions

The relevant equations for the use of atmospheric flow calculations above large wind farms in a statically neutral boundary layer will be derived in the present chapter. The general mass- and momentum laws are stated first, after which scaling is applied such that the most significant terms remain. Most theory considering conservation laws that are used in this chapter is based on [4]. The wind farm will be implemented by means of increased roughness as treated in the previous chapter, which can be added in the drag- or Reynolds stress terms in the governing equations.

3.1.1 Basic Equations

Incompressible atmospheric flow on a flat earth is determined by the following equations:

Continuity:

$$\frac{\partial u}{\partial x} + \frac{\partial v}{\partial y} + \frac{\partial w}{\partial z} = 0 \quad (16)$$

Momentum:

$$\frac{\partial u}{\partial t} + u \frac{\partial u}{\partial x} + v \frac{\partial u}{\partial y} + w \frac{\partial u}{\partial z} = -\frac{1}{\rho} \frac{\partial p}{\partial x} + 2\Omega v \sin \phi - 2\Omega w \cos \phi + F_{vx} \quad (17)$$

$$\frac{\partial v}{\partial t} + u \frac{\partial v}{\partial x} + v \frac{\partial v}{\partial y} + w \frac{\partial v}{\partial z} = -\frac{1}{\rho} \frac{\partial p}{\partial y} - 2\Omega u \sin \phi + F_{vy} \quad (18)$$

$$\frac{\partial w}{\partial t} + u \frac{\partial w}{\partial x} + v \frac{\partial w}{\partial y} + w \frac{\partial w}{\partial z} = -\frac{1}{\rho} \frac{\partial p}{\partial z} + g + 2\Omega u \cos \phi + F_{vz} \quad (19)$$

Where ρ is the air density and $\mathbf{V} = (u, v, w)$ denotes the velocity vector. The angle ϕ is the latitude, p denotes the pressure and g is the gravitational acceleration. Use is made of an orthogonal right-handed axis system which is fixed to the rotating earth, where u points in the same direction as the x co-ordinate and z is directed upwards. The viscous forces F_{vx} , F_{vy} and F_{vz} are caused by internal friction (or viscosity). For instance, F_{vx} is expressed as:

$$F_{vx} = \frac{\mu}{\rho} \left(\frac{\partial^2 u}{\partial x^2} + \frac{\partial^2 u}{\partial y^2} + \frac{\partial^2 u}{\partial z^2} \right) \quad (20)$$

The remaining shear terms (F_{vy} and F_{vz}) are of similar form.

The above set of equations gives sufficient approximation to many atmospheric flows, if the atmosphere is neutrally stable. Since static stability is a measure of the capability for buoyant convection it should be noted that net buoyant forces are only present if the earth's surface is heated or cooled. In neutral conditions the surface is neither heated nor cooled, which means that there are no vertical motions due to buoyancy. From this it may be assumed to neglect the energy equation, also referred to as 'first law of thermodynamics', when the boundary layer is in neutral conditions.

Since the main goal of this work is to examine the flow quantities in the atmospheric boundary layer above a wind farm, turbulence characteristics of the atmosphere should be modelled. Reference [6] points out that Reynolds averaging is a suitable method to solve such problems. Applying this technique, the properties u , v , w , p and ρ in the equations transform into mean and turbulent parts.

3.1.2 Scaling for Relevant Equations

In this paragraph a scale analysis is applied on the momentum equations (17-19), in which the turbulent effects of the boundary layer are included. The main goals of scaling are:

- To avoid undesired physical phenomena as, for instance, sound waves or buoyancy effects,
- To save computer time when the equations will be solved numerically.

For estimating the order of magnitude for turbulent flux terms in the surface layer it is necessary to know scale properties of large weather systems (synoptic scale). It may be expected that the scale of turbulence in the boundary layer is significantly different from that of the free atmosphere while most large-scale properties remain nearly constant. Scale properties that may change are advection terms, for instance due to changes of the earth's surface. The important scale values for this work result from observations over long periods, say, 30 years. According to [4] the following characteristic values hold for motions due to large weather systems:

Table 1: Synoptic scale properties of the most important variables

Synoptic property	symbol	scale value	unit
Horizontal velocity scale	U	10	m/s
Vertical velocity scale	W	10^{-2}	m/s
Synoptic length scale	L	10^6	m
Synoptic depth scale	H	10^4	m
Horizontal pressure difference	$\delta P/\rho$	10^3	m^2/s^2
Atmospheric scale pressure	P_0	10^5	Pa
Time scale	L/U	10^5	s
Coriolis parameter at 45° northern latitude	f_0	10^{-4}	1/s

where the Coriolis parameter f_0 is defined as $2\Omega \sin \phi$. Since weather systems at mid-latitudes are considered, an angle of 45° is assumed. In that special case the Coriolis parameter may also be defined as $2\Omega \cos \phi$. Summing up the horizontal momentum equation terms to scale:

Table 2: Scaling properties for the horizontal momentum equations

Term in momentum equation	scales	values	units
$Du/Dt, Dv/Dt$	U^2/L	10^{-4}	m/s^2
$2\Omega v \sin \phi, 2\Omega u \sin \phi$	$f_0 U$	10^{-3}	m/s^2
$2\Omega w \cos \phi$	$f_0 W$	10^{-6}	m/s^2
$(1/\rho) (\partial p/\partial x), (1/\rho) (\partial p/\partial y)$	$\delta P/(\rho L)$	10^{-3}	m/s^2
F_{vx}, F_{vy}	$(\nu U)/H^2$	10^{-12}	m/s^2

where the substantial derivative $D()/Dt$ is related to the local derivatives as $u\partial()/\partial x + v\partial()/\partial y + w\partial()/\partial z$.

The scaling results of the vertical momentum equation are summarized in table 3:

Table 3: Scaling properties for the vertical momentum equation

Term in momentum equation	scales	values	units
Dw/Dt	UW/L	10^{-7}	m/s^2
$2\Omega u \cos \phi$	$f_0 U$	10^{-3}	m/s^2
$(1/\rho) (\partial p/\partial z)$	$P_0/(\rho H)$	10	m/s^2
g	g	10	m/s^2
F_{vz}	$(\nu W)/H^2$	10^{-15}	m/s^2

From this short analysis it follows that the most important terms for large weather systems are:

- For horizontal momentum: Local acceleration, advection processes, horizontal Coriolis effects and horizontal pressure gradient,
- For vertical momentum: Gravity and vertical pressure gradient.

Since wind farms have heights that mostly are equal to the surface layer ($\approx 100\text{m}$) the equations can be simplified further. The assumptions are:

1. The vertical momentum equation is omitted: no vertical accelerations, only hydrostatic balance,
2. A two-dimensional flow will be considered ($v = 0$),
3. The flow is stationary ($\partial u/\partial t = 0$ and $\partial w/\partial t = 0$),
4. The atmosphere is in neutral conditions,
5. Turbulent exchange is the most dominant process in the atmospheric boundary layer, so the viscous terms F_{vx} , F_{vy} and F_{vz} can be neglected. Exchange of momentum due to molecular viscosity is very small compared to the exchange due to turbulent mixing. Even the synoptic scale analysis indicated that all other processes were more dominant than the viscous forces,
6. Turbulent exchange will be dominantly present within the surface layer, which means that Coriolis force and pressure gradient are of less importance on further development for that flow region (follows from scale analysis). Pressure gradient and Coriolis effects are still important to force the total boundary layer flow: this will be settled in the boundary values.

After applying assumptions 3, 4, 5 and performing Reynolds averaging on all momentum equations, equation 17 is written as:

$$\begin{aligned}
 U \frac{\partial U}{\partial x} + V \frac{\partial U}{\partial y} + W \frac{\partial U}{\partial z} + \frac{\overline{\partial u'^2}}{\partial x} + \frac{\overline{\partial u'v'}}{\partial y} + \frac{\overline{\partial u'w'}}{\partial z} = \\
 -\frac{1}{\bar{\rho}} \frac{\partial P}{\partial x} + 2\Omega V \sin \phi - 2\Omega W \cos \phi
 \end{aligned}
 \tag{21}$$

This will be the only momentum equation left if we assume two-dimensional flow. The reduction of the system of equations will be considered further in paragraph 3.3, in this section we

focus on the scaling of terms in the momentum equations. Because the turbulence intensity across the roughness change is assumed to be a step function (similar to the roughness length), horizontally homogeneous turbulence as proposed in reference [6] may be assumed. Just after the roughness change the equation becomes:

$$\underbrace{U \frac{\partial U}{\partial x} + V \frac{\partial U}{\partial y} + W \frac{\partial U}{\partial z}}_I + \underbrace{\frac{\partial \overline{u'w'}}{\partial z}}_{II} = - \underbrace{\frac{1}{\rho} \frac{\partial P}{\partial x}}_{III} + \underbrace{2\Omega V \sin \phi}_{IV} - \underbrace{2\Omega W \cos \phi}_V \quad (22)$$

Relatively close to the earth surface, the pressure gradient (term III) and the Coriolis effect (terms IV and V) can be neglected for the special case of a developing flow after a roughness change. The scaling from table 2 shows that the Coriolis effect due to the vertical velocity (term V) can be omitted because this term is at least two orders of magnitude lower than the other synoptic terms. The only term that has not been scaled is the turbulent flux term (term II). According to [4] it appears that the flux term in the atmospheric boundary layer is of the same order as the pressure gradient, Coriolis effect, advection and the local acceleration related terms. For the scaling of term II, the mixing length turbulence model is used to evaluate the turbulence flux term. It can be written as:

$$\frac{\partial \overline{u'w'}}{\partial z} = u_*^2 \left(1 + \frac{1}{z} \right) \quad (23)$$

For this term to balance advection, pressure gradient and the Coriolis effect it should at least have a scaling value of 10^{-3} m/s^2 to 10^{-4} m/s^2 . Equation 23 is valid for 100 m and less. Reference [4] assumes a u_* of 0.3 m/s as scaling value. This gives for a scale height of 100 m a value of 0.091 m/s^2 for the turbulent flux scaling value of equation 23. When a surface roughness change occur, the advection terms become larger than synoptic scale values for flow near the earth surface. The flow has to adapt to the new roughness situation and consequently the advection terms become of the same order of magnitude as the turbulent flux terms. The synoptic terms remain nearly constant because it is assumed that the larger weather patterns do not change.

3.2 Effects of Temperature and Humidity on Turbulence

Temperature and humidity are very important properties in meteorological processes. For large wind farms they can also be of significance because of their effect on the mean flow. Time constraints made it unfeasible to implement temperature and humidity into the used system of equations. Yet, to get a rough estimate for the behaviour of the wind speed above a farm due to temperature and humidity, a simple model is used. First, some physical effects of the considered properties on turbulence are explained, after which the budget equations are introduced: such equations quantify the incoming and outgoing energy or moisture considering an atmospheric volume-element. The budget equations are considered because they include effects of various processes of temperature and humidity that affect the mean atmospheric flow field. In paragraph 3.2.2 a model is considered that can easily be implemented into the system of equations and give results for temperature effects on the mean wind that qualitatively are satisfactory.

3.2.1 Physical Considerations

Temperature

In chapter 2 it was mentioned that air flowing over a rough surface causes mechanical turbulence. However, another mechanisms for the generation of turbulence exist: due to large temperature gradients near the earth's surface, parcels of air are buoyantly forced to ascent (or descent). Air parcels having higher temperatures than their surroundings are created by spatially varying soil conditions. Each soil type has its typical heat capacity, resulting in one type to heat faster than the other. The length scales of turbulence created by temperature gradient are generally larger than those due to surface friction, see reference [6]. Larger eddies enable air from greater heights to exchange momentum downwards more effectively, which tends to increase the wind velocity near the earth's surface. Above the sea surface differential heating is less significant due to the homogeneous surface and the large heat capacity; in that case convective turbulence can be caused by large differences between sea surface temperature and the air temperature of advected air masses. This creates a vertical temperature gradient near the sea surface that affects atmospheric stability considerably. Compared to land, atmospheric stability over oceans remains more constant over larger areas. From this it is concluded that turbulence above sea surfaces has a more homogeneous character than above land surfaces.

Together with temperature advection, local heating, phase-changes (e.g. evaporation, condensation), radiation and turbulent heat flux the budget equation for heat conservation describes the physical processes that were mentioned above. Reference [6] writes the budget equation, suitable to add to the system of equations 16-19, as follows:

$$\underbrace{\frac{\partial \theta}{\partial t}}_I + \underbrace{u_j \frac{\partial \theta}{\partial x_j}}_{II} = - \underbrace{\frac{1}{\rho C_p} \left(L_v E + \frac{\partial Q_j}{\partial x_j} \right)}_{III} - \underbrace{\frac{\partial \overline{u'_j \theta'}}{\partial x_j}}_{IV} \quad (24)$$

For equation 24 the Einstein summation convention is used for convenience and to save some space. Terms containing the index j must be written out. As an example, this is performed for term II: $u (\partial \theta / \partial x) + v (\partial \theta / \partial y) + w (\partial \theta / \partial z)$. Such terms must be written out similarly. Further, θ denotes the potential temperature, C_p is the specific heat of moist air for constant pressure, L_v is the latent heat of the associated phase change in [J/kg], E denotes the phase change rate (or evaporation rate) in [kg/(m³s)], Q_j represents the incoming or outgoing radiation components at the earth's surface in [W/m²]. Finally, $\overline{u'_j \theta'}$ denotes all components of the turbulent heat flux. The underbraced terms each represent a physical aspect:

- Term I denotes the local heating rate,
- Term II represents temperature gradients advected by the wind,
- Term III takes the influence of phase changes into account and
- Term IV is designated the turbulence due to heating of the earth's surface.

The effect of term IV will be adopted to build the model in paragraph 3.2.2.

Humidity

Humidity does not directly affect turbulence. However, turbulence does have a significant influence on the vertical humidity distribution. If, for instance, a considerable positive wind

gradient (as defined in chapter 2) causes mechanical turbulence in the surface layer, the air tends to become less humid near the surface and more humid at higher altitudes. Due to turbulent mixing the humidity eventually evens out across the surface layer, if no mean humidity is advected. This illustrated in figure 6.

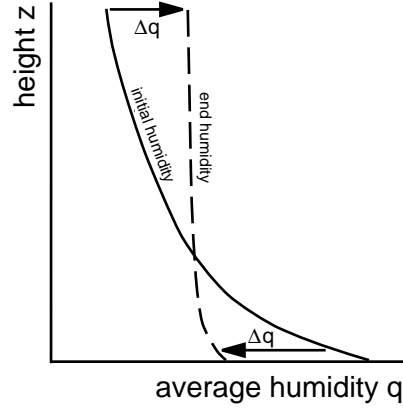


Figure 6: Influence of turbulence on the vertical humidity distribution

Due to increased turbulence within a large wind farm and the mechanism described above, extra mixing makes the humidity distribution to even out more definitely. The presence of such a farm could increase the probability of cloud forming.

To determine the effect of humidity on turbulence more accurately, reference [6] proposes the following budget equation:

$$\underbrace{\frac{\partial q_T}{\partial t}}_I + u_j \underbrace{\frac{\partial q_T}{\partial x_j}}_{II} = \underbrace{\frac{S_{q_T}}{\rho}}_{III} - \underbrace{\frac{\partial \overline{u'_j q_T'}}{\partial x_j}}_{IV} \quad (25)$$

where q_T denotes the average total moisture, S_{q_T} is a source- or sink term that represents moisture processes and $\overline{u'_j q_T'}$ is the turbulent moisture flux. The terms I and II in equation 25 represent storage and advection of moisture respectively, term III takes, for instance, evaporation of water from a falling rain drop into account and term IV represents the influence of the turbulent moisture flux on the mean total moisture. Mean total moisture includes all phase conditions of water.

Since humidity does not have a direct influence on turbulence it will not be used in the model that will be introduced in the next paragraph.

3.2.2 Artificial Solution

If the vertical momentum equation were included and a non-neutral boundary layer was assumed, the combination of equations 19 and 24 show that the mean temperature gradient is affected. This causes mean vertical acceleration of air parcels and therefore convective turbulence as already has been explained in paragraph 3.2. The exchange of momentum from higher to lower altitudes mix the air thoroughly, which causes the vertical velocity profile to become more constant with height. The effect is shown in figure 7.

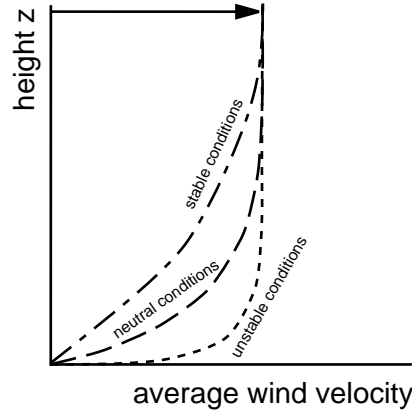


Figure 7: Influence of stability on the vertical velocity distribution

To describe the temperature effect on the wind profile, for quick results, operation on the roughness length is a true option, *ref. Corten*. The roughness length affects the turbulence intensity directly and alters the velocity profile. From figure 7 it can be concluded that the velocity profiles for stable and neutral conditions are associated to a larger z_0 , compared to unstable conditions. Since we know that the velocity profile is more constant with height for unstable conditions and that a decreasing roughness length has similar effects, we should combine a non-dimensional buoyancy term with the roughness length of a neutral atmosphere. The buoyancy term can be derived from reference [6], where the vertical momentum equation is introduced as follows:

$$\frac{\partial W}{\partial t} + U \frac{\partial W}{\partial x} + V \frac{\partial W}{\partial y} + W \frac{\partial W}{\partial z} = -\frac{1}{\rho} \frac{\partial P}{\partial z} + \underbrace{g \left(1 - \frac{\sigma_{\theta'}}{\Theta}\right)}_{\text{Buoyancy term}} + 2\Omega U \cos \phi \quad (26)$$

where $\sigma_{\theta'}$ is the root-mean-square value of the temperature deviation between the current temperature and the mean temperature and Θ is the mean temperature of the surface layer, both expressed in Kelvin.

When we multiply the 'old' roughness length by the non-dimensional part of the buoyancy term the 'new' roughness length can be defined as follows:

$$z_{0\text{new}} = z_{0\text{neutral}} \left(1 - \frac{\sigma_{\theta'}}{\Theta}\right) \quad (27)$$

Verifying this model shows that when the atmosphere is unstable, the air parcel is warmer than its surroundings, which makes the parcel to ascent. The temperature deviation therefore is positive. If the atmosphere is stable consequently the temperature deviation is negative. The roughness length decreases when the atmosphere is unstable and vice versa, which corresponds with the effect on the vertical wind profile. This indicates that the model gives qualitatively reasonable results. An brief example shows the impact on the 'neutral' roughness length: imagine a mean temperature of 293 K and an RMS value of +2 K. The neutral roughness length is estimated as 0.0001 m. According to formula 27 the 'new' roughness length becomes:

$$z_{0_{\text{new}}} = 0.0001 \times \left(1 - \left(\frac{1}{293} \right) \right) = 9.96 \times 10^{-4} \quad (28)$$

The new roughness length has decreased in comparison with the neutral value, from which can be concluded that the velocity profile reaches its constant value at lower altitude. This is in agreement with the well-known effect of the conventional definition of roughness length. The effect is further in agreement with unstable atmospheric conditions.

3.3 Physical Model for Numerical Solution

3.3.1 Model Equations

In paragraph 3.1.2 it appeared from scale analysis that, within the surface layer, the advection- and turbulent flux terms are significantly larger than the Coriolis- and pressure gradient terms, which leads to the following equations for continuity and momentum:

$$\frac{\partial U}{\partial x} + \frac{\partial W}{\partial z} = 0 \quad (29)$$

$$U \frac{\partial U}{\partial x} + W \frac{\partial U}{\partial z} = - \frac{\overline{\partial u'w'}}{\partial z} \quad (30)$$

Equations 29 and 30 determine, in this study, the flow field above a large wind farm. The boundary values on top of the boundary layer area take care of existence of the flow. The flow is driven by the pressure gradient for which is accounted by defining a U_{edge} . This property can be determined from geostrophic balance, as explained in chapter 2.

The turbulence model, to be used for equation 30, is based on mixing length theory. According to [8] the model is described as:

$$\overline{u'w'} = k^2(z + z_0)^2 \left(\frac{\partial U}{\partial z} \right)^2 \quad (31)$$

To avoid problems concerning typical values as z_0 and u_* , the governing equations will be converted into non-dimensional form. In addition a transformation of the z -coordinate will be introduced, which is useful for numerical grid purposes. The transformation is defined as:

$$\zeta = \ln \left(\frac{z + z_{01}}{z_{01}} \right) \quad (32)$$

where z_{01} denotes the roughness length of the wind farm. Substituting equations 31 and 32 into equations 29 and 30 yield:

$$\frac{\partial U'}{\partial x'} + e^{-\zeta} \frac{\partial W'}{\partial \zeta} = 0 \quad (33)$$

$$U' \frac{\partial U'}{\partial x'} + W' e^{-\zeta} \frac{\partial U'}{\partial \zeta} = 2k^2 e^{-\zeta} \frac{\partial U'}{\partial \zeta} \frac{\partial^2 U'}{\partial \zeta^2} \quad (34)$$

where $U' = U/u_*$, $W' = W/u_*$ and $x' = z/z_{01}$, as introduced by reference [8]. These are the governing equations that will be numerically solved. The solution procedure is considered in chapter 4. When solving differential equations one needs initial values and boundary conditions, which will be presented in the next paragraph.

3.3.2 Initial Values and Boundary Conditions

The physical domain on which equations 33 and 34 are solved is the x-z plane, as shown in figure 8. At $x = 0$ an initial value is given: A logarithmic velocity profile resulting from a fully developed (atmospheric) boundary layer flow field designates the starting velocity:

$$U(z) = \frac{u_*}{k} \ln \left(\frac{z + z_{00}}{z_{00}} \right) \quad \text{at} \quad x = 0 \quad (35)$$

where z_{00} is the roughness length of the freestream velocity.

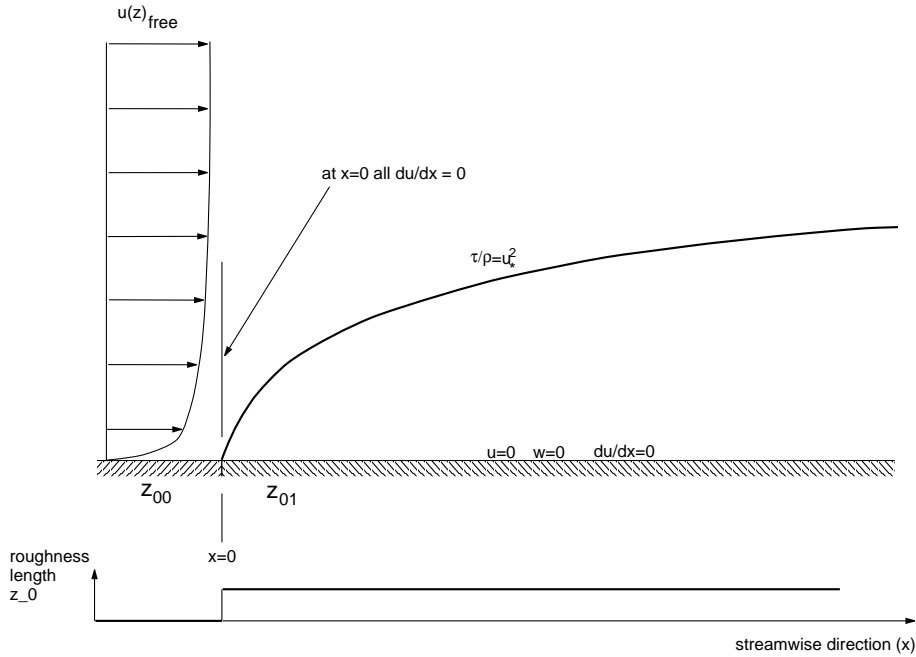


Figure 8: Initial values and boundary conditions

Further, the boundary values must be specified. Those are given at $x = 0$, $z = 0$ and at the top of the new developed boundary layer. When the flow enters the wind farm (or roughness change) the following conditions hold:

$$\frac{\partial U'}{\partial x'} = 0 \quad \text{at} \quad x = 0 \quad (36)$$

Further, at the earth's surface the vertical and horizontal velocity have vanished. Consequently, the change in horizontal velocity with respect to the x -coordinate is zero at the surface. These findings lead to the boundary conditions:

$$W' = 0 \quad \text{at} \quad \zeta = 0 \quad (37)$$

$$U' = 0 \quad \text{at} \quad \zeta = 0 \quad (38)$$

$$\frac{\partial U'}{\partial x'} = 0 \quad \text{at} \quad \zeta = 0 \quad (39)$$

Finally, the boundary condition at the upper edge of the domain is imposed by large scale weather systems. The condition is determined by geostrophic balance, which is corrected by a factor that is proportional to the turbulent drag force for the considered downstream position. The upper edge of the domain is reached when the vertical gradient of the horizontal wind velocity profile approaches zero. The boundary value can be written as:

$$\text{if} \quad \frac{\partial U'}{\partial z} \rightarrow 0 \quad \text{then} \quad U' = U'_{\text{edge}} \quad (40)$$

4 NUMERICAL MODEL

A numerical solution procedure is based on equations 33 and 34 in chapter 3. The equations are also given below:

$$\frac{\partial U'}{\partial x'} + e^{-\zeta} \frac{\partial W'}{\partial \zeta} = 0 \quad (41)$$

$$U' \frac{\partial U'}{\partial x'} + W' e^{-\zeta} \frac{\partial U'}{\partial \zeta} = 2k^2 e^{-\zeta} \frac{\partial U'}{\partial \zeta} \frac{\partial^2 U'}{\partial \zeta^2} \quad (42)$$

The turbulence model (mixing length hypothesis) introduces a non-linear set of differential equations that cannot be solved analytically. For this reason a numerical solution procedure is necessary. This chapter considers the numerical schemes and the associated numerical stability that is introduced by discretizing the governing equations. The numerical procedure is partly based on reference [8] that suggests central differencing in vertical direction. In horizontal direction this reference uses a Runge-Kutta scheme, which we replaced by an Adams-Bashforth-Moulton (ABM) method. In addition, a short verification study is performed that considers the development of the horizontal and vertical velocity. The resulting computer code is enclosed in appendix B.

4.1 Discretization of the Physical Model

Grid Transformation

The earth's surface tends to decelerate the flow in the lower parts of the boundary layer more than in the upper parts. Therefore, in the physical domain, it is necessary to use a fine grid near the surface that grows into a coarser grid at higher altitudes. Reference [5] suggests to use a rectangular grid with constant step size in time and space for the computational domain: a uniform grid simplifies the finite difference schemes. Formula 32 introduces a grid stretching transformation, which explains the $e^{-\zeta}$ terms in equations 41 and 42. Figure 9 explains the mechanism:

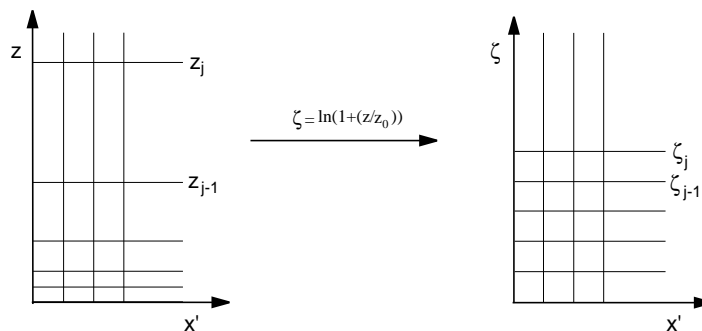


Figure 9: Grid transformation from physical domain to computational domain

Vertical Discretization

Equation 34, the momentum equation, is considered first in vertical direction. The first order differentials $\partial U'/\partial \zeta$ are replaced by central differentials:

$$\frac{\partial U'_j}{\partial \zeta} = \frac{u_{j+1} - u_{j-1}}{2\Delta\zeta} \quad (43)$$

where U' indicates the exact solution and u_{j+1} or u_{j-1} represent the numerical approximation of the non-dimensional velocity at the grid point $j + 1$ or $j - 1$. The index j suggests vertical dependence of discrete properties as velocity. The second order derivatives are represented by the following central difference:

$$\frac{\partial^2 U'_j}{\partial \zeta^2} = \frac{u_{j+1} - 2u_j + u_{j-1}}{(\Delta\zeta)^2} \quad (44)$$

Substituting the finite difference expressions into the momentum equation 34 results in an ordinary differential equation:

$$u_j \frac{du_j}{dx'} + w_j e^{-\zeta_j} \left(\frac{u_{j+1} - u_{j-1}}{2\Delta\zeta} \right) = 2k^2 e^{-\zeta_j} \left(\frac{u_{j+1} - u_{j-1}}{2\Delta\zeta} \right) \left(\frac{u_{j+1} - 2u_j + u_{j-1}}{(\Delta\zeta)^2} \right) \quad (45)$$

When the derivative du_j/dx' is isolated, it is evaluated for each $\zeta_j = \zeta_0 + j\Delta\zeta$ along a vertical line of constant x' . If at the line $x'_i = x'_0 + i\Delta x$ all derivatives are evaluated, the velocities at the next stream wise station can be determined. Equation 45 and figure 10 illustrate that three velocities from the previous position must be used to determine the velocity at the new x' position at vertical position ζ_j . The associated numerical integration procedure is introduced later.

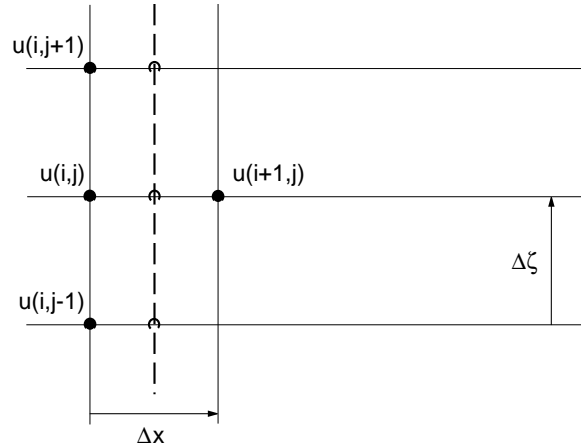


Figure 10: Computational grid and determination of velocity at new x value

At this stage the horizontal derivative cannot be determined yet since the vertical w_j velocity is unknown. The vertical velocity is obtained from the continuity equation. The difference between w_j and w_{j-1} is calculated by taking the average of the horizontal velocity gradients exactly mid point of the vertical positions j and $j - 1$. The average derivative together with the vertical velocity w_{j-1} determines the new vertical velocity at position ζ_j . Subsequently, that velocity w_j is substituted into the momentum equation. Figure 11 shows the process:

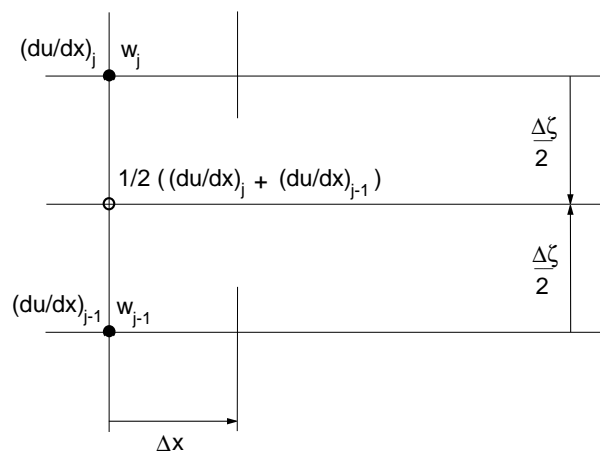


Figure 11: Calculation of the vertical velocity

The vertical velocity is determined as follows:

$$w_j = w_{j-1} - \Delta\zeta e^{(\zeta-h/2)} \frac{1}{2} \left(\frac{du_j}{dx'} + \frac{du_{j-1}}{dx'} \right) \quad (46)$$

At this stage the horizontal velocity derivatives at constant x' can be evaluated.

Numerical considerations in horizontal direction

From figure 10 can be concluded that for one new velocity $u_{i+1,j}$ three previous velocities at step i are needed: at the positions $j-1$, j and $j+1$ respectively. Numerical integration in x' direction basically is nothing more than:

$$u_{i+1,j} = u_{i,j} + \frac{du_{i,j}}{dx'} \Delta x' \quad (47)$$

where

$$\frac{du_{i,j}}{dx'} = \frac{\left(\frac{k^2 e^{-\zeta_j}}{h^3} (u_{j+1} - 2u_j + u_{j-1}) + \left(\frac{1}{4} e^{-h/2} \frac{du_{j-1}}{dx'} - e^{-\zeta_j} w_{j-1} \right) \right) (u_{j+1} - u_{j-1})}{u_j - \frac{1}{4} e^{-h/2} (u_{j+1} - u_{j-1})} \quad (48)$$

The derivative depends on the horizontal and vertical velocities and is frequently written as function:

$$\frac{du_{i,j}}{dx'} = f \left(u_{i,j+1}, u_{i,j}, u_{i,j-1}, w_{i,j-1}, \frac{du_{i,j-1}}{dx'} \right) \quad (49)$$

which clearly demonstrates the dependences of the derivative.

Due to accuracy and stability the ABM method is chosen. Reference [1] defines the associated equations. The predictor formula (the Adams-Bashforth part) is written as:

$$u_{i+1}^* = u_i + \frac{\Delta x}{24} (55u'_i - 59u'_{i-1} + 37u'_{i-2} - 9u'_{i-3}) \quad (50)$$

where $()' = d/dx ()$.

The derivative at the next step becomes:

$$u'_{i+1} = f(x_{i+1}, u_{i+1}^*) \quad (51)$$

The corrector step (the Adams-Moulton part) is:

$$u_{i+1} = u_i + \frac{\Delta x}{24} (9u'_{i+1} + 19u'_i - 5u'_{i-1} + u'_{i-2}) \quad (52)$$

The method is based on fitting interpolation polynomials. In this case, 4 horizontal velocity derivatives with respect to the horizontal coordinate are used for a (third degree) polynomial fit. Realising that the velocity at the next station ($i + 1$) has to be determined, the ABM method needs four previous horizontal velocity derivatives, starting at the present station i . The predictor formula 50 gives an estimate for the horizontal velocity at station $i + 1$, which is used by formula 51 for evaluating the derivative at the station $i + 1$. Eventually, the derivative at $i + 1$ and the corrector formula 52 determine the final value of u_{i+1} at vertical level j . For the ABM method to perform the integration from i to $i + 1$ two function evaluation are necessary: equations 50 and 51.

From equation 50 can be deduced further that this method cannot be applied too close to the initial conditions. The first steps indicated as $i - 3$, $i - 2$, $i - 1$ and i , must be calculated by a one-step method that has a similar local truncation error is the ABM method. If station $i - 3$ represent the initial condition, the Runge-Kutta (RK) scheme determines the properties for the remaining three stations.

Runge-Kutta needs 4 function evaluations for one integration step. This can be illustrated by writing down the scheme:

$$\begin{aligned} k_1 &= f(x_i, u_i) \\ k_2 &= f\left(x_i + \frac{1}{2}\Delta x, u_i + \frac{1}{2}k_1\Delta x\right) \\ k_3 &= f\left(x_i + \frac{1}{2}\Delta x, u_i + \frac{1}{2}k_2\Delta x\right) \\ k_4 &= f(x_i + \Delta x, u_i + k_3\Delta x) \end{aligned} \quad (53)$$

The RK method calculates the slope at the starting point (i), at two mid points ($i + 1/2$) and at the end point $i + 1$ for each step. The new velocity is calculated from the previous velocity by giving each new determined slope (indicated by k_i) its own weight as written below:

$$u_{i+1} = u_i + \frac{\Delta x}{6} (k_1 + 2k_2 + 2k_3 + k_4) \quad (54)$$

Finally, it is worth mentioning that the RK method has not been used to evaluate the complete problem because twice as much function evaluations for one integration step are necessary.

4.2 Numerical Stability and Accuracy

In the previous paragraph it was mentioned that the Adams-Bashforth-Moulton (ABM) scheme together with the Runge-Kutta scheme is used due to favourable accuracy and stability properties. In this section accuracy and stability is considered in more detail.

Accuracy

Reference [1] shows that the ABM method has a local truncation error of $O(\Delta x)^5$. To start the numerical integration process three integration steps must be evaluated by a one step method. The Runge-Kutta scheme was chosen because the local truncation error is of the same order of magnitude. If the ABM method is applied after the maintains a local truncation error of $O(\Delta x)^5$

Stability

Since the numerical integration methods consist of explicit schemes (i.e. one new value result from one or more previous horizontal step values), it must be noted that there are restrictions for the step size in horizontal and vertical direction. The horizontal grid is limited by the vertical step size. The vertical step is considered first: it seems to be related to the roughness length of a wind farm. The difference between the surface (ζ_0) and the first level (ζ_1) gives the result:

$$\zeta_1 - \zeta_0 = \Delta\zeta = \ln\left(\frac{z_{01}}{z_{01}} + 1\right) = \ln 2 \approx 0.7 \quad (55)$$

if the first level represents the roughness length. It is allowed to define a vertical step size that is smaller than $\Delta\zeta = \ln 2$, however, if $\Delta\zeta \leq 0.35$ one should be aware of instabilities propagating in ζ and x' direction. Larger step sizes then $\Delta\zeta = 0.7$ do not represent the sharp wind gradient near the surface sufficiently, which result in less accurate solutions of the velocity field.

For choosing a step size in x direction, the solution remains stable if:

$$\Delta x \leq \frac{c}{\|\lambda_{\max}\|} \quad (56)$$

where c denotes a constant that results from the integration scheme and λ_{\max} is the largest eigenvalue of the matrix that is built when the system of equations is linearized. Since time constraints do not allow us to linearize the system, an indication of the stability condition for the Euler scheme is used to estimate the largest step size in x direction:

$$\Delta x \leq \frac{1}{2}(\Delta\zeta)^2 \quad (57)$$

The problem arising when using this criterion is that the condition is valid for linear differential equations. As a matter of fact, the present system of non-linear equations should be linearized after each step in Δx . This results in a stability condition that constantly changes and so does the maximum step size. In the present problem, due to time constraints, the step size is not changed, which causes a chance that the solution becomes unstable (far) downstream of the roughness change.

4.3 Short Model Verification

To verify the physical and mathematical correctness of the model, a uniform velocity distribution will be tested as artificial initial condition. The development of the horizontal flow is analysed and the vertical velocity is checked in correspondence with characteristic growth of an (internal) boundary layer. The uniform wind is expected to decelerate near the surface and not to change at the top of computational domain. In between, the distribution of the horizontal velocity will tend to an exponential shape. Figure 12 shows the horizontal flow field in x direction:

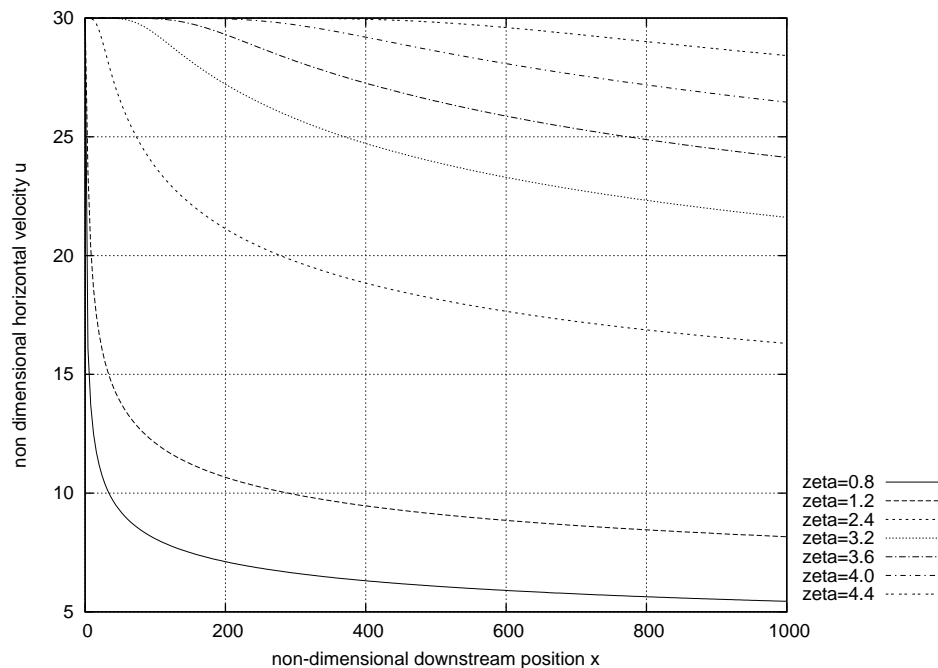


Figure 12: Development of horizontal velocity from uniform initial velocity profile

The vertical velocity is expected to be the largest near the roughness change: there the boundary layer growth is at maximum. More downstream, the vertical velocity decreases because the flow is finding a new equilibrium for the horizontal wind speed, if no more roughness changes occur. Consequently, the vertical velocity approaches a constant value, depending on the vertical co-ordinate. In horizontal direction the vertical velocity decreases, which coincides with the fact the the boundary layer height becomes constant when the horizontal velocity finds its new equilibrium value. The vertical velocity field in streamwise direction has characteristics as illustrated in figure 13:

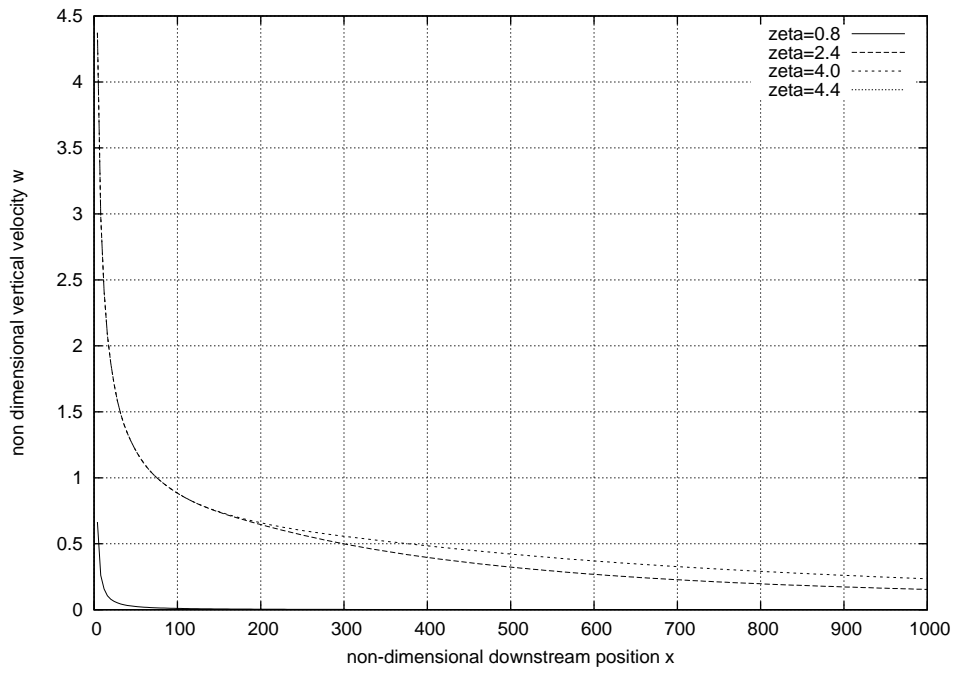


Figure 13: Development of vertical velocity from uniform initial velocity profile

5 RESULTS AND VALIDATION

5.1 Boundary Layer at Sea

Horizontal Velocity Development in Downstream Direction

Figure 14 summarizes the measurements together with several model runs. The measurements are indicated as single points and the model results as lines. The measurement results are introduced in an other report that is part of this project as well.

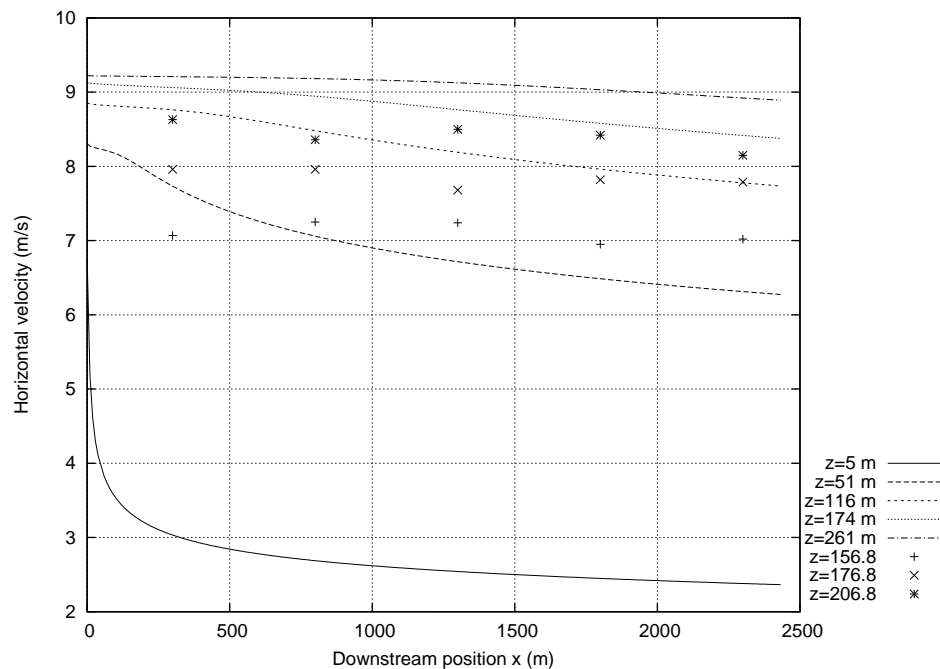


Figure 14: Development of horizontal velocity field

Before analysing the data, some additional information concerning the measurements and model runs are necessary:

- Since the model approaches wind farms as a smeared-out roughness length it is expected that the velocity field below approximately hub height (i.e. 106.8 m) is not representative for a description of the actual velocity field.
- All distances and heights are converted into 'real' properties: each length or height is multiplied by 400.
- The validation will emphasize the velocity field at and above hub height, up to a maximum of $\zeta = 4.8$ for the computational model. The farm roughness length $z_{01} = 2$ m.
- The model calculations for sea are performed for the heights 5 m, 51 m, 116 m, 174 m and 261 m.
- The measurements give results for x values of 300 m, 800 m, 1300 m, 1800 m and 2300 m downstream of the first wind turbine at heights of 156.8 m, 176.8 m and 206.8 m.

- The model calculation results are non-dimensional. The actual velocities are determined by estimating the u_* from the wind tunnel measurements. For the present sea boundary layer $u_* = 0.267$ m/s was estimated.

Using this information, the following can be said concerning the measurements in comparison with the computational model:

- The wind tunnel measurements give lower velocity results than the numerical model. A plausible reason could be that the 'scale factor' u_* was overestimated.
- The development of the measured horizontal velocity tends to behave similar as the numerical model indicates. However, the horizontal velocity decay is less pronounced in the measurements. It could be caused by a pressure gradient in flow direction in the wind tunnel. Atmospheric boundary layers in general do not clearly notice a pressure gradient in flow direction as large as is present in a wind tunnel.
- According to the numerical model, the 'equilibrium velocity' near the surface will be reached after 2500 meters (=25D). At higher altitudes it takes more time. The calculation was performed until approximately 25D because of numerical stability problems and show that equilibrium is reached at larger distances than near the surface. In other words: if the turbine distance (at hub height) is 6D, it appears that the velocity is still decreasing at 24D (i.e. at the fifth turbine). This could be an indication of the power development in large wind farms in downstream direction.

Velocity Profiles

Due to the increased roughness the horizontal velocity decreases, which is compensated by the vertical velocity field within the new boundary layer as verified in chapter (4). Measurements show a velocity deficit due to the wind turbine rotor, see figure 15.

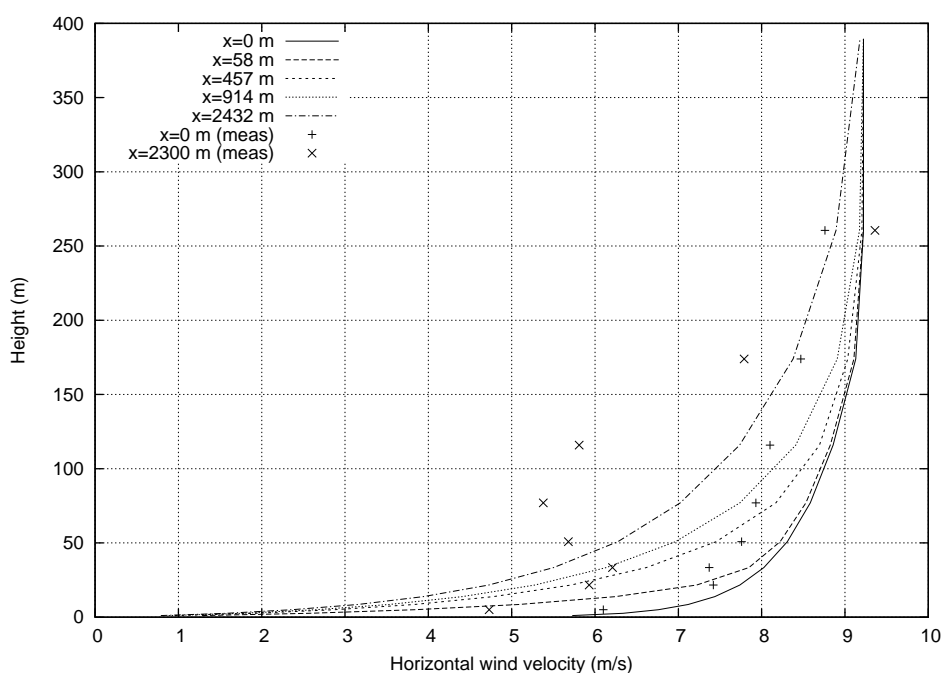


Figure 15: Vertical distribution of horizontal velocity field, at several downstream positions

The measured velocity profile does not appear in numerical model results, because of smearing out turbine wake effects in the roughness length. Therefore, a quantitative comparison between numerical model and measurements is not very useful at and below hub height. At the top of the rotor (i.e. 156.8 m which coincides with $\zeta = 4.3$ for sea roughness) some comparison can be performed. The measurements indicate that, above the wind farm, the wind velocity in the tunnel increases in streamwise direction while the numerical model maintains constant wind velocity. This difference originates from the pressure gradient in the wind tunnel versus the atmospheric conditions. It should be noted that the atmospheric model contains a pressure gradient term in flow direction which has been set to zero for atmospheric boundary layer conditions. Figure 15 shows the velocity profiles for different x positions.

The numerical solution of a wind profile in the far wake does not take local wake effects into account. However, the effect of smearing out wind farms in the surface roughness results in a significant deceleration of the flow. This effect is also felt at hub height, however, the profile does not show a wake-characteristic shape. Actual wind turbine wakes show a velocity deficit behind the turbine that is caused by a resultant drag force working at the center of the rotor, that causes the flow to decelerate most in that center (and at the Earth's surface, because of turbulent surface drag). The numerical model output can be thought as an averaged wind profile due to the total of wind farm- and surface roughness. Choosing for this view, the model output is suitable for roughly estimating the power of turbines that are positioned in the very far wake.

5.2 Boundary Layer over Land

Horizontal Velocity Development in Downstream Direction

For analysing the data much of the information in paragraph 5.1 can be used. The additional information for the land boundary layer measurements and calculations are given below:

- The validation will emphasize the velocity field at and above hub height, up to a maximum of $\zeta = 4.4$ for the computational model. The farm roughness length $z_{01} = 2$ m.
- The model calculations for sea are performed for the heights 6 m, 27 m, 63 m, 95 m, 143 m and 215 m.
- The measurements give results for x values of 300 m, 800 m, 1300 m, 1800 m and 2300 m downstream of the first wind turbine at heights of 156.8 m, 176.8 m and 206.8 m.
- The model calculation results are non-dimensional. The actual velocities are determined by estimating the u_* from the wind tunnel measurements. For the present land boundary layer $u_* = 0.375$ m/s was estimated.

Globally, the same conclusions for the boundary layer over land can be drawn. Measurements behave quantitatively more like the the model results, which is probably caused by a better estimation of u_* . The results are plotted in figure 16.

Velocity Profiles

The same arguments for a boundary layer over land are true. The measured and calculated initial velocity profile coincides very well, which indicates that the estimation of u_* is correct. The results can be found in figure 17.

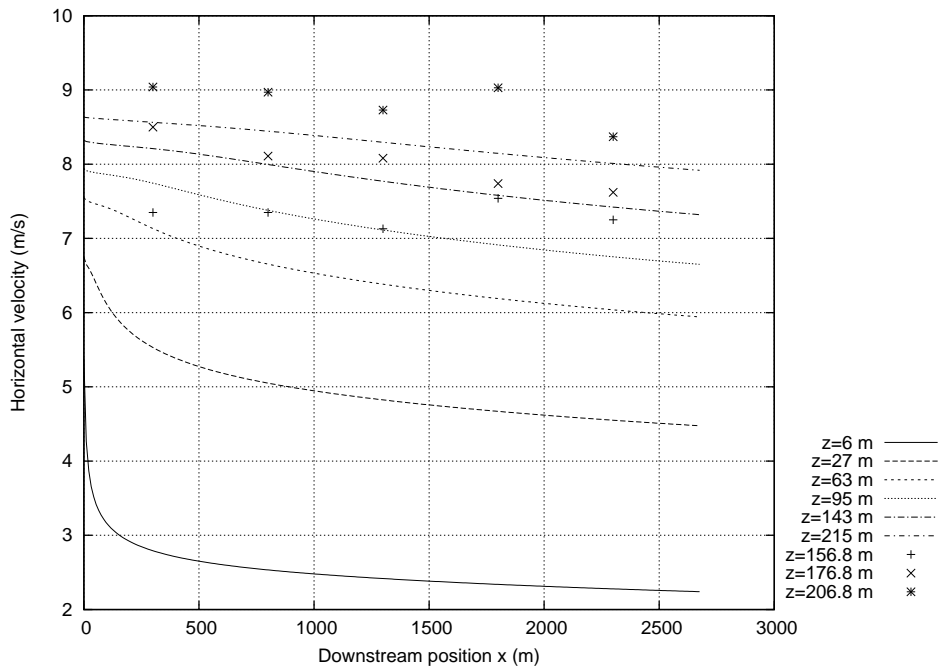


Figure 16: Development of horizontal velocity field, the points represent the wind tunnel measurements over land

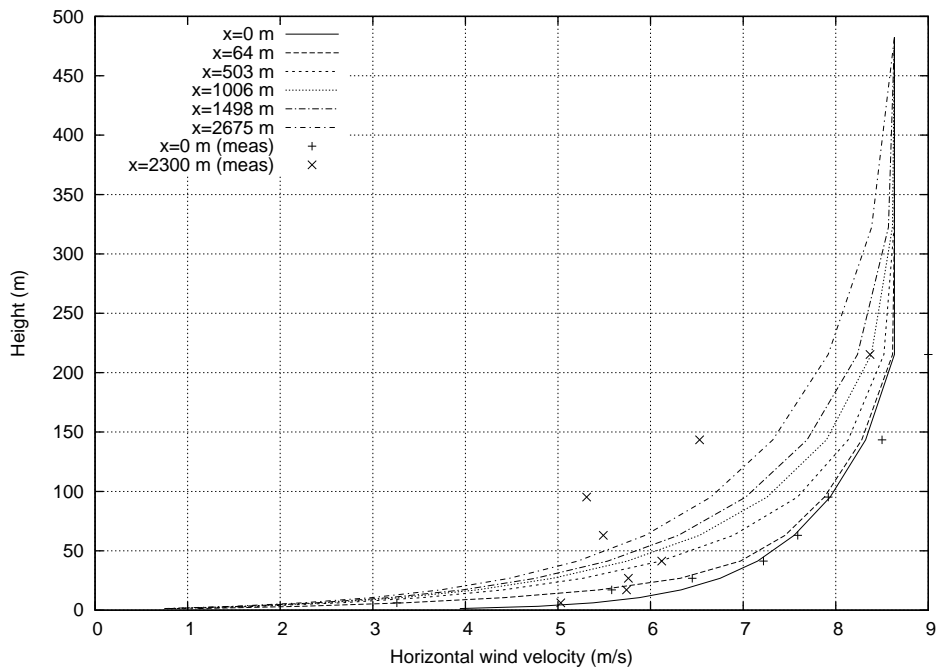


Figure 17: Vertical distribution of horizontal velocity field, at several downstream positions

5.3 Conclusions

Considering the measurements and calculations, in general the computational model tends to decay the horizontal velocity field to slowly. The code can be used to estimate the behaviour of large wind farms in the far wake and at higher altitudes, say, from the top of the turbine including rotor. Estimating the friction velocity u_* from measurements must be performed carefully, because it is not sure whether the wind tunnel generates a correct logarithmic profile that corresponds with a boundary layer over sea. The velocity profiles that result from the theoretical model do not generate a velocity deficit, because the wind turbine farm is integrated into the roughness length. The surface generates a force that is assumed to remain constant with increasing altitude (up to 100 m, within the surface layer) which causes the wind profile to be logarithmic. It should be noted that the considered profile is decelerated more near the surface in comparison with a method where the turbine drag is applied in the center of the rotor. Then, the Reynolds stress due to the surface remains constant that causes the normal velocity gradient near the surface and the (discrete) rotor drag force causes the velocity deficit. Finally, the model can be used as estimator for the behaviour of turbines in large wind farms at far wake positions.

6 CONCLUSIONS AND RECOMMENDATIONS

6.1 Conclusions

The main conclusion of this work is that the wind velocity does not reach its equilibrium value after 5 turbines as suggested by classical wind farm codes like FYNDFARM. The computational model resulting from this project suggests that, at hub height and beyond, the velocity still decays after the fifth wind turbine.

In addition, the results of the measurements and calculations made us conclude that a considered turbine in the far wake experiences the local wake of the neighbouring turbine rows (referred to as 'turbine wake'). All turbine rows in front of, say 2 rows, can be modelled as surface roughness. The resulting velocity profile from that roughness length is referred to as 'wind farm wake'. The considered turbine experiences the velocity profile from the wind farm wake and from the turbine wakes.

The above manner to calculate velocity profiles for a turbine in the far wake may be used in programs as FYNDFARM, however, other methods are also suitable to improve existing computer codes.

6.2 Recommendations

The computational model is a step in the right direction for improving wind farm power calculations. However, there are many issues that have to be improved:

- Extend the computer code to 3D flow, i.e., add momentum equations into x , y and z direction,
- Include the first law of thermodynamics,
- Replace the mixing length theory by a 'two-equation model' like a $k - \epsilon$ model,
- Include moisture for possible cloud forming.

REFERENCES

- [1] William E. Boyce and Richard C. DiPrima. *Elementary Differential Equations and Boundary Value Problems*. John Wiley & Sons, United States, 1995.
- [2] A. Crespo. Modelization of a large windfarm considering the modification of the atmospheric boundary layer. In *European Wind Energy Conference*, Nice, France, 1999. p1109-1112.
- [3] Sten Frandsen. On the wind speed reduction in the centre of large clusters of wind turbines. *Journal of Wind Engineering and Industrial Aerodynamics*, pages 251–265, 1992.
- [4] James R. Holton. *An Introduction to Dynamic Meteorology*. Academic Press, Seattle, Washington, U.S.A., 1992.
- [5] John D. Anderson (jr.). *Computational Fluid Dynamics*. McGraw-Hill, United States, 1995.
- [6] Roland B. Stull. *An Introduction to Boundary Layer Meteorology*. Kluwer Academic Publishers, Dordrecht, The Netherlands, 1988.
- [7] Roland B. Stull. *Meteorology Today for Scientists and Engineers*. West Publishing Company, United States, 1995.
- [8] P.A. Taylor. On wind and shear stress profiles above a change in surface roughness. *To be published*, 1968.

A INITIAL PAPER

T. Hegberg and P.J. Eecen

Energy research Centre of the Netherlands, Petten, the Netherlands

Ph. +31224564798, Fax +31224568214, E-mail hegberg@ecn.nl

2002 Global Windpower Conference (Paris, April 2-5), carrying the title:

THE EFFECT OF LARGE WIND FARMS ON THE ATMOSPHERIC BOUNDARY LAYER

A.1 Introduction

This paper deals with large wind farms and how they possibly affect the atmospheric boundary layer (ABL). In the future many large wind farms will be installed offshore. An offshore wind farm results in considerable roughness change in relation to the sea surface. This causes a significant change in windspeed and wind direction within a wind farm, which could have significant consequences for the park lay-out. This was already pointed out in reference [1]. However, the treatment was not entirely clear. In section two and three this method will be described. In section four a different method will be treated.

In order to determine the effect in reference [1], first an artificial roughness length of the wind farm has to be determined. Then we have a look at the development of the internal boundary layer (i.b.l.) as a result of the roughness change of the wind farm. With that information the turbulent drag force will be calculated, in order to determine the new equilibrium situation in the wind farm. From that equilibrium the new wind speed and wind direction is calculated, that are quite different from the conditions outside the wind farm.

A.2 Roughness Length of a Wind Farm

To determine the change in wind speed and wind direction the roughness change must be determined. Because the wind farm is located at sea the undisturbed roughness, characterised by its roughness length $z_{0,1}$, is very low. We assumed that due to the roughness change caused by the wind farm the boundary layer wind adapts immediately. The wind farm results in a roughness length according to reference [1], of:

$$z_{0,2} = h_t e^{-\frac{\kappa}{\sqrt{c_t + \kappa^2 I_0^2}}} \quad (58)$$

where $z_{0,2}$ is the roughness in the wind farm, h_t is the hub height of the turbines, κ is the Von Karman constant, c_t is a macro wake effect and I_0 is the undisturbed turbulence intensity.

Next, the unknowns in equation (58) will be considered: c_t and I_0 . For c_t we need the thrust coefficient C_T curve and the spacing between the turbines (reference [1]).

$$c_t = \frac{\pi C_T}{8s^2} \quad (59)$$

The non-dimensional spacing s of the turbines in equation (59) (reference [1]) is

$$s = \sqrt{\frac{A}{D^2}} \quad (60)$$

where $A = \frac{\text{Total area of the windfarm}}{\text{Total number of turbines}}$ and D denotes the rotor diameter. What is left to determine is the undisturbed turbulence intensity. We consider a neutral boundary layer for which the turbulence intensity is

$$I_0 = \frac{1}{\ln\left(\frac{h_t}{z_{0,i}}\right)} \quad (61)$$

If we include atmospheric stability, equation (61) must be adapted. In this article a neutral atmospheric boundary layer is assumed. Because we have a description of the artificial roughness length in a large wind farm the roughness change is also known. In the next section the effects of roughness changes are treated.

A.3 Surface Parameters Due To a Roughness Change

At a point where the roughness length changes, a new boundary layer starts to develop. This means that characteristic values like z_0 and u_* obtain a different value. Generally a wind velocity profile is assumed (reference [2]):

$$v(z) = \frac{u_{*i}}{\kappa} \left(\ln\left(\frac{z}{z_{0,i}}\right) - \Psi_i \right) \quad (62)$$

where u_{*i} , $z_{0,i}$ and Ψ_i are the friction velocity, the roughness length and the scale height of the i -th internal boundary layer. For each set of surface parameters an approximate boundary layer height is determined. That is called the scale height H . This parameter is an indication of turbulence at the surface. When there is a high turbulence level, the scale height increases and vice versa. The scale height is to be determined as follows (reference [2]):

$$H = c_H \frac{u_{*i}}{f} \quad (63)$$

where f is called the Coriolis parameter, and C_H is a constant with a value between 0.25 and 0.35.

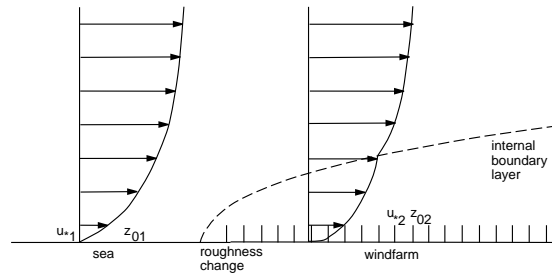


Figure 18: Development of the internal boundary layer over a large wind farm

Above the internal boundary layer the wind profile remains unchanged as indicated in figure 18. Within the i.b.l. the profile has changed. This means that the turbulent drag forces increase due to the growth of the i.b.l. Once the final height of the i.b.l. is known one can make an estimation of the turbulent drag force. This ‘drag’ determines the new equilibrium of the atmospheric forces. After the roughness change due to the wind farm the friction velocity changes and due to that change we get a different turbulent drag force. The drag force forms

a new equilibrium with other atmospheric forces, which can be noticed in the wind velocity change and the wind direction change.

A.4 Estimating the Wind Vector

If the boundary layer thickness increases, the drag force change is also noticeable at larger heights. As a result, the average drag force changes within the total boundary layer and becomes larger downstream in the wind farm. From elementary meteorology we know that horizontal equilibrium in the boundary layer is made between three forces: the pressure gradient force, the Coriolis force and the turbulent drag. The turbulent drag force and the Coriolis force cause the wind velocity vector to make an angle with respect to the isobars, which is illustrated in figure 19.

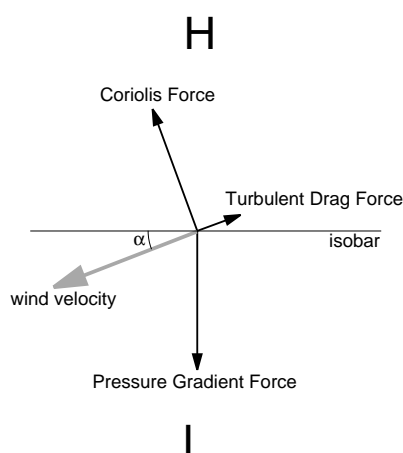


Figure 19: Force equilibrium in freestream condition

When the roughness changes, for example due to the presence of an offshore wind farm the turbulent drag force changes. Here we assume the wind farm is infinitely large and the drag force obtains its new equilibrium value. The force equilibrium rearranges itself, the velocity angle increases and the wind velocity decreases, according to figure 20.

The next question to rise could be: How much will the wind direction and the wind velocity change due to the presence of a wind farm? To give global results, one could perform a global calculation of the wind velocity and the wind direction based on the force equilibrium in the different boundary layers. First we assume that both layers are fully developed. For this, we assume that the pressure gradient force and the Coriolis force are constant over the entire boundary layer thickness. The turbulent drag force gets an average value over the boundary layer thickness. The three forces now get their value. The pressure gradient force is written as:

$$F_G = \frac{1}{\rho} \frac{\partial p}{\partial x} \quad (64)$$

where ρ is the air density and $\frac{\partial p}{\partial x}$ denotes the pressure gradient. For the Coriolis force we have:

$$F_C = 2v\Omega \sin \phi \quad (65)$$

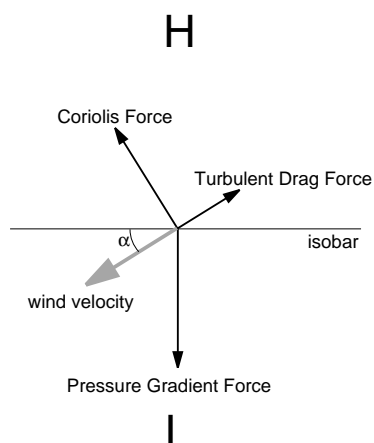


Figure 20: Force equilibrium over the wind farm

where Ω is the angular velocity of the earth, v is the wind velocity, and ϕ is the latitude. For the turbulent drag force we assume the following, according to reference [3]:

$$F_T = \frac{C_D}{H} v^2 \quad (66)$$

In this equation C_D denotes the drag of the earth surface, H is the height of the atmospheric boundary layer and v is the wind velocity.

Since we have the values and directions of the forces, an equation of the following form is deduced:

$$\left(\frac{C_D}{H}\right)^2 v^4 + 4\Omega^2 v^2 \sin^2 \phi = \frac{1}{\rho^2} \left(\frac{\partial p}{\partial x}\right)^2 \quad (67)$$

Solving this equation leads to the wind velocity. The angle α is determined as follows. From figure 19 or 20 it follows that:

$$\frac{F_C}{F_G} = \frac{2\rho v \Omega \sin \phi}{\frac{\partial p}{\partial x}} = \cos \alpha \quad (68)$$

From this equation follows that if the wind velocity decreases and the Coriolis factor, the pressure gradient, and the air density remain unchanged, the cross isobaric flow angle increases (assuming that the angle is less than 90 degrees).

A.5 Results

In this section we provide an indicative calculation of the effect of a roughness change at sea due to a wind farm, so that we get an idea of the amount of change in wind velocity and wind direction due to the presence of an offshore wind farm.

The following specifications of the park are assumed:

The following meteorological data are needed:

Total area of wind farm	36×10^6	m^2
Number of turbines	121	-
Hub height	100	m
Rotor diameter	100	m
Thrust coefficient at rated power	0.7	-
Roughness of sea surface	0.005	m

Von Karman constant	0.4	-
Air density	1.225	kg/m^3
Pressure gradient	1.5×10^{-3}	Pa/m
Earth angular velocity	7.29×10^{-5}	rad/s
Thickness of ABL.	1000	m
Latitude of wind farm	53	$^{\circ}\text{N}$

The drag coefficients of the surfaces are for the ocean 0.001 and for the offshore wind farm 0.009, taken at $h=100$ m. These values are based on the different roughness lengths. The drag coefficients are calculated with a formula for a neutral boundary layer:

$$C_{\text{DN}} = \frac{\kappa^2}{\ln^2\left(\frac{z}{z_0}\right)} \quad (69)$$

where C_{DN} means the drag coefficient in the neutral boundary layer.

From the above data the wind speed becomes 10.47 m/s with a cross isobaric flow angle of 5° . In the wind farm the velocity becomes 8.72 m/s with a cross isobaric flow angle of 34° . Thus the velocity decreases with 1.75 m/s and the angle changes about 29° .

However, over the oceans the boundary layer thickness is smaller. This gives a larger difference in wind velocity and a larger cross flow angle between the freestream and the wind farm. If we assume a boundary layer thickness of 500 m, the undisturbed values are for the wind speed 10.35 m/s and for the cross flow angle 10° . Over the wind farm (assuming that the new boundary layer is fully developed) the wind speed is reduced to 7.09 m/s and the cross flow angle increases to 48° . The wind speed now reduces with 3.26 m/s and the angle increases with 38° . A boundary layer thickness of 500m is not uncommon at the North Sea.

A.6 Conclusions

The results of the (rough) calculations presented in this paper indicate that a large wind farm has a significant influence on wind conditions within the wind farm. The calculations show that a large offshore wind farm has a significant effect on the wind velocity and wind direction. The effect even becomes larger when the boundary layer thickness is smaller. Naturally, the dimensions of the wind farm have a significant effect: when the dimensions of the wind farm decrease, the effects become less. A more accurate calculation should be performed to determine a more detailed effect on the park lay-out. It is clear that the wind conditions due to a roughness change will have a significant effect on the park lay-out, especially when the atmospheric boundary layer is stable.

References

1. Crespo A. et al., March 1999, "Modelization of a Large Wind Farm Considering the Modification of the Atmospheric Boundary Layer", European Wind Energy Conference, Nice, France.
2. Han van Dop, Maart 2002, "ECN Cursus Grenslaagmeteorologie", Universiteit van Utrecht, Nederland.
3. Stull, Roland B., 1995, "Meteorology Today for Scientists and Engineers", University of Wisconsin-Madison and University of British Columbia, St. Paul, Minnesota, USA.

B COMPUTER CODE

```

Option Explicit
'*****
'
' Velocity field in horizontal en vertical direction
' Written 26/11/03 by T. Hegberg
' Revised 08/12/03 by T. Hegberg
' Revised 13/12/03 by T. Hegberg
' Revised 27/12/03 by T. Hegberg
' Revised 08/01/04 by T. Hegberg
'
'This program calculates the velocity field in horizontal and vertical direction.
'The subroutines "Runge-Kutta" and Adams-Bashforth-Moulton" are used to calculate the
'development of the flow in downstream (x) direction.
'
'*****

Dim h As Double           'Step size in vertical zeta direction
Dim z00 As Double        'Roughness length of freestream
Dim z01 As Double        'Roughness length of wind farm
Dim hulp As Double       'Used as help variable
Dim rhulp As Double      'Used as help variable
Dim dx As Double         'Step size in streamwise direction
Dim term_1 As Double     'Used as help variable
Dim term_2 As Double     'Used as help variable
Dim term_3 As Double     'Used as help variable
Dim term_4 As Double     'Used as help variable
Dim x0 As Double         'Initial co-ordinate in streamwise integration:
                        'x0=0
Dim x As Double          'Dimensionless co-ordinate in x-direction
Dim zeta(0 To 200) As Double 'Transformed vertical co-ordinate
Dim z(0 To 200) As Double 'Dimensionless vertical co-ordinate before
                        'transformation ln(z/z0+1).
                        'Transformation is used to create a rectangular
                        'grid with constant step sizes.
Dim dudx(0 To 4, 0 To 200) As Double 'Derivative of hor. Velocity u w.r.t. streamwise
                        'direction x. Indices:(i-streamwise, j-zeta
                        'direction)
Dim u(0 To 5, 0 To 200) As Double 'Horizontal velocity(i-streamwise, j-vertical
                        'zeta)
Dim w(0 To 4, 0 To 200) As Double 'Vertical velocity(i-streamwise, j-vertical
                        'zeta)
Dim i As Long            'Step index in streamwise direction
Dim j As Long            'Step index in zeta direction
Dim m As Long            'Maximum steps in x-direction
Dim n As Long            'Maximum steps in zeta-direction
Dim step As Long         'Used as help variable

Const karman = 0.4

Sub snelheidsveld()
'*****
'Here the program starts
'*****

x0 = 0                    'Set horizontal and vertical coordinates
zeta(0) = 0              'to zero
h = Range("E13")         '.....
dx = Range("E16")        'Input must be given in the Excel sheet
z00 = Range("E4")        '
z01 = Range("E10")       '
n = Range("E14")         '
m = Range("E15")         '
step = Range("H16")      '.....

Application.ScreenUpdating = False

'initial velocity at x=0-----

```

```

For j = 1 To n + 1
    zeta(j) = zeta(0) + j * h
    z(j) = z01 * (Exp(zeta(j)) - 1)
    dudx(4, j) = 0
    u(5, 0) = 0
'
'   u(5, j) = 30
'
    If z(j) < 200 Then
        u(5, j) = (1 / karman) * Log((z01 / z00) * (z(j) / z01) + 1)
    Else
        u(5, j) = (1 / karman) * Log((z01 / z00) * (200 / z01) + 1)
    End If
Next

'Numerical solution method in streamwise direction-----

For i = 0 To m
    x = x0 + i * dx
    u(0, 0) = 0
    u(1, 0) = 0
    u(2, 0) = 0
    u(3, 0) = 0
    u(4, 0) = 0
    u(5, 0) = 0
    w(0, 0) = 0
    w(1, 0) = 0
    w(2, 0) = 0
    w(3, 0) = 0
    w(4, 0) = 0
    dudx(0, 0) = 0
    dudx(1, 0) = 0
    dudx(2, 0) = 0
    dudx(3, 0) = 0
    dudx(4, 0) = 0
    If i <= 4 Then
        Runge_Kutta
    Else
        Adams_Bashforth_Moulton
    End If
Next

Application.ScreenUpdating = True

End Sub

Sub Runge_Kutta()
'*****
'The fourth order Runge-Kutta method evaluates the derivatives once at the initial
'points, twice at the midpoints and once at the end point. The obtained derivatives
'are weighted averaged and the final end point is calculated by means of the mean
'derivative.
'*****
For j = 1 To n
    Call derivs(u(5, j + 1), u(5, j), u(5, j - 1), zeta(j), w(4, j - 1),
                dudx(4, j - 1), dudx(4, j))
    Call vert(dudx(4, j), dudx(4, j - 1), w(4, j - 1), zeta(j), w(4, j))
Next

For j = 1 To n

```

Turbine Interaction in Large Offshore Wind Farms

```
    u(4, j) = u(5, j) + 0.5 * dx * dudx(4, j)
                                                    'step
Next
For j = 1 To n
    Call derivs(u(4, j + 1), u(4, j), u(4, j - 1), zeta(j), w(3, j - 1),
                dudx(3, j - 1), dudx(3, j))
                                                    'Second
                                                    'derivative
    Call vert(dudx(3, j), dudx(3, j - 1), w(3, j - 1), zeta(j), w(3, j))
Next
For j = 1 To n
    u(3, j) = u(5, j) + 0.5 * dx * dudx(3, j)
                                                    'step
Next
For j = 1 To n
    Call derivs(u(3, j + 1), u(3, j), u(3, j - 1), zeta(j), w(2, j - 1),
                dudx(2, j - 1), dudx(2, j))
                                                    'Third
                                                    'derivative
    Call vert(dudx(2, j), dudx(2, j - 1), w(2, j - 1), zeta(j), w(2, j))
Next
For j = 1 To n
    u(2, j) = u(5, j) + dx * dudx(2, j)
                                                    'step
Next
For j = 1 To n
    Call derivs(u(2, j + 1), u(2, j), u(2, j - 1), zeta(j), w(1, j - 1),
                dudx(1, j - 1), dudx(1, j))
                                                    'Fourth
                                                    'derivative
    Call vert(dudx(1, j), dudx(1, j - 1), w(1, j - 1), zeta(j), w(1, j))
Next
For j = 1 To n
    u(0, j) = u(5, j) + (dx / 6) * (dudx(1, j) + 2 * dudx(2, j) + 2 * dudx(3, j) +
    If Abs((1 / h) * (u(0, j) - u(0, j - 1))) < 2 Then 'Upper boundary condition
        u(0, j) = u(5, j)
    End If
    Cells(20 + j, 1) = zeta(j)
    If i = 0 Then
        Cells(20, 2) = i * dx
        Cells(20 + j, 2) = u(5, j)
    Else
        hulp = i / step
        rhulp = Int(hulp)
        If Abs(rhulp - hulp) <= 0.0001 Then
            Cells(18, 2 + rhulp) = rhulp
            Cells(19, 2 + rhulp) = i
            Cells(20, 2 + rhulp) = step * rhulp * dx
            Cells(20 + j, 2 + rhulp) = w(1, j)
        End If
    End If
Next
For j = 1 To n
    u(5, j) = u(0, j)
Next
End Sub

Sub Adams_Bashforth_Moulton()
'*****
'Multistep integration method using Adams-Bashfort predictor formula and
'Adams-Moulton corrector formula:
'Gives (num). stable solutions if step-length is sufficiently small and is faster
'than Runge-Kutta. The first of three steps are calculated with Runge Kutta
```

```

'because of the initial values cannot be calculated with a fifth order multistep
'method.
'*****
For j = 1 To n
    u(1, j) = u(5, j) + (dx / 24) * (55 * dudx(1, j) - 59 * dudx(2, j)
        + 37 * dudx(3, j) - 9 * dudx(4, j))
        'Predictor
        'step
Next

For j = 1 To n
    Call derivs(u(1, j + 1), u(1, j), u(1, j - 1), zeta(j), w(0, j - 1),
        dudx(0, j - 1), dudx(0, j))
        'Evaluation of
        'derivative
    Call vert(dudx(0, j), dudx(0, j - 1), w(0, j - 1), zeta(j), w(0, j))
Next
'for corrector formula

For j = 1 To n
    u(0, j) = u(5, j) + (dx / 24) * (9 * dudx(0, j) + 19 * dudx(1, j)
        - 5 * dudx(2, j) + dudx(3, j))

    If Abs((1 / h) * (u(0, j) - u(0, j - 1))) < 2 Then
        u(0, n) = u(5, j)
    End If

    dudx(4, j) = dudx(3, j)
    dudx(3, j) = dudx(2, j)
    dudx(2, j) = dudx(1, j)
    dudx(1, j) = dudx(0, j)

    Cells(20 + j, 1) = zeta(j)

    hulp = i / step
    rhulp = Int(hulp)
    If Abs(rhulp - hulp) <= 0.0001 Then
        Cells(18, 2 + rhulp) = rhulp
        Cells(19, 2 + rhulp) = i
        Cells(20, 2 + rhulp) = step * rhulp * dx
        Cells(20 + j, 2 + rhulp) = w(0, j)
    End If
Next

For j = 1 To n
    u(5, j) = u(0, j)
Next

End Sub
-----
Function derivs(uhp As Double, u As Double, uhm As Double, zeta As Double,
    whm As Double, dudxhm As Double, dudx As Double) As Double
'*****
'This function determines the derivative needed for the numerical integration
'routines that solve differential equations, for instance Runge-Kutta
'*****
Dim term_1 As Double 'Used to avoid numerical difficulties with processor accuracy
Dim term_2 As Double 'The formula has been "divided" into 4 parts
Dim term_3 As Double '
Dim term_4 As Double '
Dim dpdx As Double ' pressure gradient in flow direction can be chosen

dpdx = Range("L3")

term_1 = uhp - uhm
term_2 = uhp - 2 * u + uhm
term_3 = ((1 / h) ^ 3) * (karman ^ 2) * Exp(-zeta) * term_1 * term_2
term_4 = 0.25 * Exp(-0.5 * h) * dudxhm - (0.5 / h) * Exp(-zeta) * whm
dudx = (term_3 + term_4 * term_1 - dpdx) / (u - 0.25 * Exp(-0.5 * h) * term_1)

End Function

```

Turbine Interaction in Large Offshore Wind Farms

```
Function vert(dudx As Double, dudxhm As Double, whm As Double, zeta As Double,
             w As Double) As Double
'*****
'This function is used for determining de deriv function at a point i,j.
'The vertical velocity is calculated, which depends on the derivative du/dx at a
'point i,j-1 and i,j.
'*****

w = whm - 0.5 * h * Exp(zeta - 0.5 * h) * (dudx + dudxhm)

End Function
```

	Date: August 2004	Report No.: ECN-C-04-033	
Title	Turbine Interaction in Large Offshore Wind Farms		
Author	T. Hegberg, G.P. Corten, P.J. Eecen		
Principal(s)	Novem		
ECN project number	7.4170		
Principal's order number	2020-01-13-10-004		
Programmes			
Abstract			
<p>This report presents a relative simple numerical model in which the wind farm is modelled as surface roughness. Model results suggest that the wind velocity decreases even for large downstream distances in wind farms (further than the 5th-10th row). As a consequence, the power production far downstream decreases more than classical wind farm wake codes assume (Assumed was, that the wind velocity reached its equilibrium value at the 5th row). In principal, the computational model assumes a neutrally stable atmosphere. The present model is extended with a slight vertical temperature gradient dependence, which is implemented in the surface roughness. This allows velocity field solutions that hold for atmospheric conditions including slight departures from neutral atmosphere.</p> <p>The validation has been carried out using wind tunnel measurements. For that purpose, technically very advanced 1:400 scale model turbines were designed. They also can be used for other purposes than atmospheric boundary layer experiments. The validation suggests that the wind velocity has not reached its equilibrium value after 5 rows, which indicates that the numerical model can be used for global studies of atmospheric flows above (and behind) large wind farms.</p>			
Keywords			
wind energy, wind turbines, wind farms, atmospheric boundary layer, numerical methods			
Authorization	Name	Signature	Date
Checked	A.J. Brand		
Approved	G.P. Corten		
Authorised	H.J.M. Beurskens		